LBL-28078

Lawrence Berkeley Laboratory
UNIVERSITY OF CALIFORNIA

CELL & MOLECULAR BIOLOGY DIVISION

# The LET Dependence of Interphase Chromosome Breakage and Rejoining in Two Mammalian Cell Lines

Edwin Goodwin
(Ph.D. Thesis)



December 1988

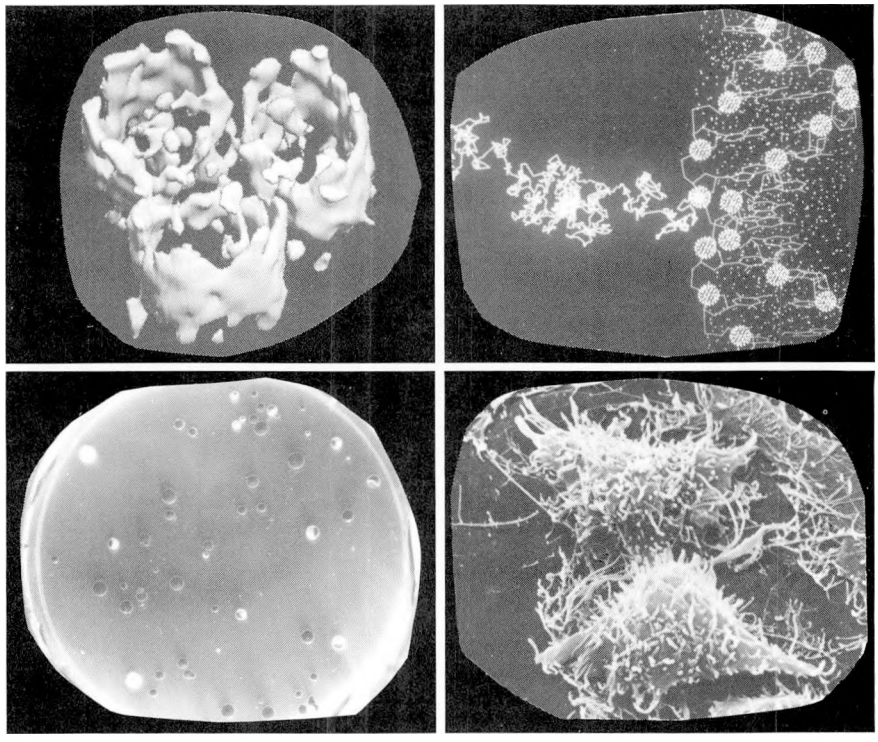

Prepared for the U.S. Department of Energy under Contract Number DE-AC03-76SF00098

## DISCLAIMER

LBL--28078

DE91 016270

# The LET Dependence of Interphase Chromosome Breakage and Rejoining in Two Mammalian Cell Lines

Edwin Goodwin
Ph.D. Thesis

Biophysics Graduate Group
University of California

and

Cell and Molecular Biology Division
Lawrence Berkeley Laboratory
University of California
Berkeley, CA 94720

December 1988

This work was supported by the National Institutes of Health under Contract No. NIH-RR-05918, the National Cancer Institute under Contract No. NCI-CA-15184, and by the Director, Office of Energy Research, Office of Health and Environmental Research, Division of Health Effects, of the U.S. Department of Energy under Contract No. DE-AC03-76SF00098.

# THE LET DEPENDENCE OF INTERPHASE CHROMOSOME BREAKAGE AND REJOINING IN TWO MAMMALIAN CELL LINES

Edwin Goodwin

## ABSTRACT

Chromosomal breakage and rejoining was examined in the $G_1$-phase of a Chinese hamster ovary (CHO-tsH1) cell line using a technique known as premature chromosome condensation. The initial level of breakage was measured in cells exposed to x-rays and 9 particle beams covering a LET range of more than 3 orders of magnitude (from 0.56 to 2700 keV/μm). The rate and extent of rejoining of interphase chromosome breaks was measured in cells exposed to 4 particle beams having LET values from 0.56 to 183 keV/μm. Cell survival dose-response curves were obtained for x-rays and 4 particle beams having LET values in the range of 1.5 to 2700 keV/μm. The average number of chromosome breaks per cell was observed to be linearly proportional to the dose of low-LET x-rays or high-LET Ar, Ne or Nb ions. The initial level of breakage per unit dose was found to be LET-dependent. Expressed as a RBE, the yield of breaks rose from a plateau at the lowest LET values to a peak in the 100-200 keV/μm range and then continuously declined thereafter, eventually falling well below the low-LET plateau. A maximum RBE of 1.5 was observed at 183 keV/μm. The survival RBE vs LET curve was qualitatively similar but the amplitude of the curve depended on the survival level chosen in computing the RBE. The average number of chromosome breaks per particle traversal of the cell nucleus rose steadily from ~0.006 to 11 breaks/cell as the LET increased from 0.56 to 2700 keV/μm. Chromosome breaks were Poisson distributed within the $G_1$-phase cell population after exposure to low LET radiations. The distribution of breaks became progressively overdispersed with increasing LET most likely as the result of multiple chromosome breakage produced by single particle traversals of the cell

nucleus. The rate of rejoining of interphase chromosome breaks showed no clear LET dependence. However the proportion of apparantly nonrejoining breaks (those which remain after long repair intervals) was observed to be LET-dependent, increasing nearly 4-fold as the LET rose from 0.56 to 183 keV/μm. Experiments were also conducted with a human/hamster hybrid cell line, UV24C2-3, exposed to x-rays and a Neon-ion particle beam (LET = 183 keV/μm). Results confirmed both a RBE of 1.5 and also a larger proportion of nonrejoining breaks for the Ne-ion exposures compared to x-rays. Chromosomal misrepair was investigated by scoring prematurely condensed ring chromosome aberrations in $G_1$-phase UV24C2-3 cells . After x-rays the average number of rings per cell increased with time. The data could be fitted well by assuming first order kinetics for the misrepair process. The maximum number of rings formed after long repair times could be fitted to a quadratic dose response. Compared to the x-ray results, far fewer rings formed after a Ne-ion dose that produced the same initial number of chromosome breaks. Results from the thesis research suggest that the LET dependence of the survival response is influenced by three facets of chromosomal damage and repair: 1. A LET-dependent variation in the efficiency per unit dose for initial chromosome breakage, 2. A distribution of breaks that becomes progressively overdispersed with increasing LET, and 3. A LET-dependent increase in the proportion of nonrejoining chromosome breaks.

TABLE OF CONTENTS

ACKNOWLEDGEMENTS

I find myself at a threshold: behind, the student years are coming to an end; ahead, I hope a productive career in science. Looking back and feeling a deep sense of gratitude, I would like to acknowledge some of the individuals who have influenced my graduate training and research. I wish to thank:

Dr. Cornelius Tobias for taking me on as a graduate student, for sharing your profound insights into the field of radiation biology and for giving me the freedom to pursue my own research interests. You taught me that science can always be fresh and exciting;

Dr. Eleanor Blakely for generously offering help on a great number of occasions and for collaborating on the chromosomal misrepair experiments. From you I learned that optimism and persistence are what drive science;

Dr. Edward Alpen for advice and for serving on both the qualifying exam and dissertation committees. It was in your class that I first developed an interest in radiation biology;

Dr. Max Alfert for serving on the dissertation committee and for several interesting discussions;

Dr. Michael Cornforth and Dr. Joel Bedford for teaching me the PCC technique. Without your help the research reported here might never have been attempted;

Dr. Lawrence Thompson for providing the cell lines used in the experiments;

Dr. Daniel Pinkel for teaching me the technique of fluorescently staining labeled DNA probes following *in situ* hybridization;

Polly Chang and Lori Lommel for teaching me sterile cell culture methods and for assisting with many experiments;

Kathy Bjornstad for helping with a number of experiments;

Dr. Michael Yezzi for sharing his experience with the CHO cell lines and for teaching me the method of cell synchrony by mitotic selection;

Gayla Ivery for assistance with experiments, especially those involving the effects of cycloheximide and fluorescent staining of hybridized probes;

Dr. Teresa Patterson for suggesting the use of a drawing tube apparatus as an aid in counting chromosome fragments;

The Bevelac operating crew for technical expertise in accelerator operations; and

Lilian Hawkins and Geree Williams for an excellent job of typing the thesis.

To those mentioned and many others who have helped along the way: Your guidance, assistance and encouragement have brought me to this threshold; the knowledge you have taught me carries me beyond it into my future.

The following grants have provided financial support for me or my research: NIH-RR-05918, NCI-CA-15184 and DOE-DE-AC03-76SF00098.

# OVERVIEW AND GOALS

The absorption of energy from a beam of ionizing radiation can lead to a number of well-defined biological alterations in cellular properties. The best characterized of these alterations, loss of clonogenic potential, has been linked to mitotic dysfunction brought about by the acquisition of certain kinds of chromosome aberrations (see Review). Mutation and transformation have also been linked to chromosomal misrepair although the evidence here is not yet as strong. These traditional biological endpoints of radiation action are the results of a damage and repair/misrepair process that has been completed long before the biological change is measured. Even chromosome aberrations are not scored until the first post-irradiation mitosis which, for $G_1$ cells, can be 12 to 24 hours after the initial radiation exposure. In 1974 a new technique known as "premature chromosome condensation (PCC)" was introduced into the study of radiation effects. The PCC technique made it possible to detect chromosome breaks in individual interphase cells at a time when repair processes are still at work. This assay offers the most direct means available for examining damage and repair at the chromosomal level. At the time of the initiation of the thesis research, the PCC technique had not been applied in a systematic investigation of LET-dependent chromosomal breakage and rejoining in $G_1$-phase cells. The undertaking of such a study became the focus of the thesis research and was motivated by a desire to better understand the high-LET-induced lesions that affect cell survival. Availability of a wide variety of high-energy particle beams accelerated by the Bevalac at Lawrence Berkeley Laboratory made the research possible. The thesis research had these specific goals: to determine the LET dependence of 1) the initial yield of chromosome breakage in the $G_1$-phase of two mammalian cell lines, 2) the distribution of these breaks

in the irradiated cell population, 3) the rate and maximum extent of chromosome break rejoining by cellular repair processes, and 4) the rate of formation and maximum yield of ring chromosome aberrations. With this knowledge in hand, the final goal was to make comparisons to survival data obtained under similar circumstances in a search for insights into the mechanisms underlying variations in the survival response of cells exposed to radiations of differing LET.

# GENERAL REVIEW

## Physics of Charged Particle Irradiations

When a heavy charged particle passes through matter it loses kinetic energy via electromagnetic interactions with electrons in the medium being traversed. The interactions of primary importance include ionizations, electronic excitations and, where the incident particle velocity is high enough, Cerenkov radiation. The rate of energy loss is not constant, but rather it increases as the particle slows. This observation was first reported by Sir William Bragg in 1913. The plot of relative ionization vs depth of penetration is nov known as the Bragg ionization curve. A mathematical expression for the rate of energy loss is given by the Bethe-Block stopping power equation (Evans, 1955). The phenomenon of greater energy deposition with depth of penetration provides the essential rationale underlying clinical trials with heavy-ion charged particle beams. The concept of linear energy transfer (LET), which is defined as the quantity of energy absorbed "locally" by the medium being traversed, was introduced by Zirkle et al (1952) to present a clear distinction to "stopping power", the rate of energy loss by the particle. Sufficiently energetic secondary electrons (delta rays) may travel a distance from their point of origin that brings them, and the energy they deposit, outside of (or into) a critical volume of interest, usually the cell nucleus. The concept of restricted LET was introduced in an attempt to reduce the ambiguity of the phrase "locally deposited energy" by restricting the range of electron energies to be included in the calculation of LET (International Commission on Radiological Units Report No. 16, 1970). Thus the value $LET_{300}$ includes the energy of all secondary electrons with initial energies of 0 to 300 eV. When electrons of all energies are to be included the subscript "$\infty$" is used. Often, as will be done in this thesis, the subscript "$\infty$" is

omitted after a first mention. The concept of restricted LET has not found much use in the field of charged particle radiobiology.

The spatial pattern of energy deposition about the particle trajectory is called "track structure". In their model of track structure Chatterjee et al. (1973), Chatterjee and Magee (1980), and Chatterjee and Schaefer (1976) distinguish between two distinct concentric radial energy-density domains, the core and penumbra. Slightly more than half of the energy transferred in each track segment is located in the inner core region while the remainder is deposited in the penumbra, the outer region beyond the core radius bounded by the maximum range of free energetic electrons created by ionizations in the core. LET is determined by the electron density and average ionization potential of atoms in the medium being traversed, and by the charge and velocity of the projectile particle at each point in its trajectory. The radial dimensions of the core and penumbra depend only on the nature of the medium and the projectile velocity, but not on particle charge. For this reason a small, slow-moving charged particle can have an LET equal to that of a much heavier, faster moving particle. The track structures corresponding to the fast and slow particles will, however, be quite different. For the same LET the lighter, slower particle will have smaller core and penumbra radii, but a higher linear energy density within these two regions. Most of the particle beams used in the thesis research had track core diameters comparable in size to the width of a chromatin fiber (110Å) while the size of the penumbra covered many cell diameters.

Another approach to the problem of track structure is due to Dr. Robert Katz and coworkers (1978). In their analysis the radial dose distribution is calculated in a complex manner by combining experimental data with theoretical and empirical relations. An interesting feature of

the model is an inseparable intertwining of a description of track structure and the properties of the detector used in assessing energy deposition patterns. Although predictions of this model are qualitatively similar to those of Chatterjee et al., Katz feels that the separation of track structure into a core and penumbra is artificial and unjustified.

To be of interest to the biomedical community, a charged particle beam must be capable of penetrating tissue to a substantial depth to reach the internal site of a tumor. A particle in one of these high velocity beams possesses a kinetic energy well in excess of that required to overcome Coulomb repulsion to bring it and a stationary nucleus in its path into a realm where the nuclear force predominates. The resulting interaction may cause the fragmentation of the projectile nucleus, the target nucleus, or both (Curtis and Schimmerling, 1977). As a beam of charged particles penetrates to greater depths, nuclear collisions cause a progressive loss of primary particles from the beam accompanied by a shower of secondary particles of increasing relative intensity. The beam becomes a complex mixture of primary and secondary particles of different energies that changes from point to point along the Bragg curve. It becomes necessary to use a beam-average LET weighted either by dose (dose-averaged LET) or by particle fluence (track-averaged LET). In this thesis the dose-averaged LET is used exclusively.

Cell Survival vs LET,

In the mid 1950's Puck and Marcus (1956) perfected the colony formation assay as a measure of reproductive integrity in mammalian cells exposed to ionizing radiation. Since that time cell survival has remained a major, and certainly the most frequently measured, biological endpoint for the investigation of radiation effects. The review presented here will be concerned with the influence of LET on mammalian

cell survival and will be organized roughly according to particle beam irradiations of increasing charge and energy.

Barendsen et al. (1963, 1966) exposed T1 cells, a permanent cell line of human origin, to 150 kVp x-rays, electrons, and low energy cyclotron-accelerated γ-particles and deuterons. The LET range varied from 0.3 to 166 keV/μm. The relative biological effectiveness (RBE), which is a ratio of doses at an isosurvival level between a reference radiation (x-rays) and a particle beam radiation, was plotted vs LET. They found a slow rise in RBE as the LET increased to 10 keV/μm and a more rapid rise beyond. A maximum effectiveness was found at ~ 100-110 keV/μm. Beyond that point the RBE declined. The position of the peak did not depend on the survival level chosen to calculate the RBE. Survival curves became exponential as the LET reached and then exceeded the value at the RBE peak. Although the position of the RBE peak on the LET axis was independent of survival level, the magnitude of the peak was found to decrease with decreasing survival. Berry (1977), using murine lymphocytic leukemia P-388 cells exposed to low energy helium and Boron ions, found a peak RBE in a lower LET range (60-80 keV/μm). Madhvanath et al. (1976) obtained a similar result using human lymphocytes. Hall et al. (1975) obtained qualitatively similar results by irradiating Chinese hamster cells with neutrons of different energies.

Using T1 cells and Chinese hamster M3-1 cells, Todd (1964) studied the effect on survival of low energy charged particles ranging from He to Ar. In both cell lines a peak RBE was found at 220 keV/μm. Survival curves were exponential starting from a point just before the peak and continuing into the high LET range. Cox et al. (1977) also working with human cells (diploid fibroblasts) and hamster cells (V79), looked at survival RBE's in the 20 to 470 keV/μm range obtained by accelerating He, B and N ions. They saw a peak RBE in a range of ~ 85 to 200 keV/μm.

Skarsgard et al. (1967) found a peak RBE in the 100 to 200 keV/μm range after exposure of hamster cells ($CH2B_2$) to irradiation by charged particles from He to Ar.

Blakely et al. (1979) and Tobias et al. (1984) exposed T1 cells and a radiation-sensitive human diploid cell line (AT-2SF) to x-rays and to high energy C, Ne and Ar ions. They found a peak RBE at ~ 140 keV/μm for the T1 cells. The peak RBE for the sensitive AT-2SF cells was less pronounced and occurred at a slightly lower LET. Their data indicated track structure effects with slower particles of a lower charge being more effective than faster, more highly charged particles of the same LET. Because of this, RBE became a multiple-valued function of LET above 100 keV/μm. Three variables, such as dose, LET and charge, were necessary to uniquely characterize the survival response. Kraft et al. (1985) exposed V79 cells to a wide variety of particles (from He to U) over a broad range of energies. Their results demonstrate a separation in the RBE vs LET curve according to particle charge in the very high LET range. The individual branches of the RBE curve have been called "hooks" because of their appearance. Hooks are another indication of track structure effects on survival.

The ability of cells to recover from radiation exposure, demonstrated by an increase in survival with post-irradiation incubation, is known as potentially lethal damage (PLD) repair (Phillips and Tolmach, 1966). Plateau-phase Chinese hamster ovary (CHO) cells exhibited PLD repair after low LET x-ray or $^{60}Co$ irradiations but not after exposure to fast neutrons (7 and 21 MeV, LET = 70 and 50 keV/μm) or to α-particles (100 keV/μm) (Gragg et al., 1977; Raju et al., 1977). Confluent mouse embryo C3H 10T½ cells exposed to high energy C, Ne and Ar beams with LET values ranging from 10 to 105 keV/μm did show PLD repair, but somewhat less than after x-rays (Ngo et al., 1980). The same cells did not repair

damage induced by low energy Ar ions (8.3 MeV/u, 1500 keV/μm). Human T1 cells repaired x-ray PLD but did not show PLD repair after Bragg peak Ne exposures (183 keV/μm) in early $G_1$ phase (Blakely et al., 1985). Later in $G_1$ the T1 cells did repair some Ne damage.

The work reviewed here clearly demonstrates a variation in cell-killing effectiveness by radiations differing in LET. Because of track structure effects, LET alone was not sufficient to uniquely characterize the survival response for all particles. A satisfactory description of survival required the use of both the particle charge and energy, or parameters derived from them. Each study found a peak in the RBE vs LET curve, however, the LET at the peak position varied considerably. Progress in understanding the cellular response to charged particle irradiation is slowed by limitations inherent in the survival assay. Survival is, at a minimum, a two-stage process. In the first stage the absorption of energy initiates physical and chemical changes resulting in biological damage. The cell attempts to remove this damage in the second stage through enzymatic-repair pathways. The survival response will depend on the types and quantities of initial damage and on the effectiveness of the cellular repair system. The limitation of the survival assay is that it can reveal only the end result of the two-stage process; the acquisition or avoidance of acquiring a lethal lesion. New techniques capable of dissecting damage and repair processes at the subcellular and molecular levels will be required to gain useful insights into the survival response of cells exposed to charged particle beams.

Chromosome Aberrations

Radiation has long been known to produce large numbers of chromosome aberrations in cycling cell populations. Furthermore, it was demonstrated many years ago (Sax, 1941) that cells containing aberrant chromosomes are selectively eliminated from proliferating cell systems.

This observation led to the hypothesis that chromosome aberrations are responsible for loss of cellular reproductive capacity following exposure to ionizing radiation. Puck (1958) irradiated exponentially growing human euploid cells with 230 kVp x-rays and then tested for both survival and chromosome aberrations. His data were interpreted as supporting the chromosomal damage hypothesis of cell lethality. Using Chinese hamster cells (lines DON and CHO), Dewey et al. (1971) x-irradiated synchronized cells at several points in the cell cycle and applied various post-irradiation treatments. In this way cell survival was made to vary by a factor of 4. Measurements of chromosomal aberrations were performed under the same conditions. At the 37% survival level they observed an average of ~ 1 exchange or deletion-type aberration per cell. This strong correlation between chromosome aberrations and cell death was maintained throughout the cell cycle. Carrano (1973) and Carrano and Heddle (1973) studied the fate of visible chromosome aberrations and were able to derive formulae to predict the transmission of these defects into future mitotic generations. Their results provide further quantitative evidence of the deleterious effects on cellular viability of asymmetrical chromosome exchanges and chromosome deletions. Other aberrations such as translocations and inversions, which are not seen or scored except by special techniques, apparently do not lead to nonviability. Grote et al. (1981) and Joshi et al. (1982) followed individual Syrian Hamster BHK cells under phase-contrast microscopy after exposure to x-rays in the $G_1$ phase of the cell cycle. This method allows the detection of acentric fragments (chromosome deletions) as micronuclei in live cells during any interphase following the first post-irradiation mitosis. Cells with micronuclei almost always showed a deterioration in reproductive capacity that resulted in either stop-growth (79%) or slow-growth (21%) colonies.

Dicentric chromosomal bridges were observed to frequently break during the interphase following the first mitosis.

Giles and Tobias (1954) observed RBE values greater than 1 for chromosome aberration induction in Tradescantia microspores exposed to 190 MeV deuterons and 380 MeV α-particles. After exposure to x-rays, γ-rays and fast neutrons, Conger et al. (1958), also using Tradescantia, found maximum RBE values of 8 for chromosome and 11 for chromatid aberrations in the 50 to 70 MeV/μm range. Roberts and Holt (1985) examined both the induction of chromosome aberrations and cell killing in Syrian hamster cells after exposure to γ-rays, x-rays and neutrons of two energies (15 and 2.1 MeV). For each of these radiations they found a good correlation between the surviving fraction and the proportion of mitotic cells not containing a visible chromosome aberration. Their data on the yields of dicentrics and also acentric chromosome fragments could be fitted to a linear-quadratic-dose dependence. For dicentrics, the coefficient of the dose-squared term decreased with increasing LET. For acentric fragments the linear term increased with increasing LET. Dicentrics followed a Poisson distribution in the irradiated cell population for each radiation quality while acentric-fragments were found to be overdispersed. Skarsgard et al. (1967) measured the yield of chromosome aberrations as part of a LET study using low energy heavy-ion particle beams. The LET range of this study spanned 3 orders of magnitude from ~ 2 to 2000 keV/μm. A close parallel was found between the RBE vs LET responses for aberration production and cell survival. They interpret their results as supporting the hypothesis that the radiosensitive sites for chromosomal damage and cell lethality are the same. Sabatier et al. (1987) evaluated chromosomal lesions induced by γ-rays, neutrons and Ne ions. Irradiations were performed on non

cycling, $G_0$ human lymphocytes and aberrations were scored in R-banded metaphase chromosomes. Compared to $\gamma$-rays, the high LET radiations induced more breaks per abnormal mitosis and more complex rearrangements. Geard (1985) examined the production of chromosome aberrations in V79 cells irradiated in all phases of the cell cycle over a range of 10 to 80 keV/μm. Aberrations were most frequent in cells irradiated in $G_2$ at all LET values. S phase was the least sensitive. $G_1$ had an intermediate sensitivity, but was closer to the S phase response. The yield of aberrations showed a linear dose response for irradiations of $G_1$ and S-phase cells but was curvilinear with positive curvature for $G_2$ cells. The variation in the yield of aberrations through the cell cycle diminished at higher LET values. As the LET increased by a factor of 8 the frequency of aberrations increased 4 fold when measured per unit dose or 32 fold when measured per unit fluence. Comparing chromosome aberrations formed in exponentially growing V79 cells exposed to either 300 rad of x-rays or 500 rad of 400 MeV/u uranium ions (LET = 2600 keV/μm), Kraft et al. (1985) observed a shift in the frequency of aberration types away from a preponderance of asymmetrical exchanges at low LET to mostly chromosome fragments at high LET. After exposure to uranium ions a new type of aberration appeared. Observed as extensive damage to a single chromosome, the new aberration was called "chromosome disintegration". Ritter et al. (1987) found a linear increase in the number of chromosome disintegrations in V79 cells with increasing fluence of particles from a 28 MeV/u Kr beam, while total chromosome aberrations followed a nonlinear curve having negative curvature. Also seen by Ritter et al. was a RBE vs LET relationship very similar to that for intracellular DNA double strand breakage obtained by Aufderheide et al. (1987) and Kampf and Eichhorn (1983).

The studies reviewed here establish a strong positive correlation between certain chromosome aberration types (asymmetrical exchanges and deletions) and loss of cellular proliferative capacity. Puck (1958) suggested that cell death results from either a loss of genetic information due to failure of an acentric fragment to segregate properly in anaphase of mitosis or to failure of two daughter cells to separate following telophase due to the presence of a dicentric chromosome bridge. The term "mitotic-death" has been invented to describe this mechanism of cell lethality. In some cell lines an "interphase death" has also been observed (Little and Nagasawa, 1985). In this case a cell dies before reaching a first post-irradiation mitosis.

Although research has clearly demonstrated the ability of ionizing radiation to generate chromosomal defects, the physical and biological processes involved are still largely unknown. Two competing hypotheses have arisen. The first originated with Stadler (1931) and was promoted by Sax (1940). In their "breakage first" hypothesis, radiation produces breaks in interphase chromosomes. Over a period of time the breaks are rejoined by a cellular repair process. Occasionally two chromosome ends created at different break points are mistakenly joined. The result is observed as an exchange-type aberration in mitosis. The failure of a break to rejoin results in a chromosomal deletion. The second major hypothesis of aberration formation is due to Revell (1955) and is known as the "exchange hypothesis." In Revell's view, radiation induces a lesion in interphase chromosomes. The type of lesion was unspecified other than that it is not a chromosome break. Exchanges can occur when two closely-spaced lesions are being simultaneously repaired. A break is observed when an exchange is incomplete. In the exchange hypothesis, breakage is caused by the cellular repair system, while the breakage

first hypothesis asserts that breakage is the direct result of the action of radiation.

The nature of the initial radiation-induced lesion whose misrepair eventually results in the formation of chromosome aberrations is still the subject of controversy. Natarajan and Obe (1978) introduced neurospora endonuclease into permeablized x-irradiated CHO cells. A large increase in chromosome aberrations was observed, presumably due to conversion of single-strand DNA breaks into double-strand breaks by the endonuclease. Bryant (1984) treated permeablized V79 cells with restriction enzymes. He found that the blunt-ended double-strand breaks produced by PVUII were very effective at inducing aberrations. Bam H1, which produces double-strand breaks with overlapping single-stranded ends, resulted in very few aberrations. Natarajan and Obe (1984) have confirmed and extended Bryant's findings. Preston (1982) observed an increase in x-ray-induced dicentrics in human leukocytes after treatment with cytosine arabinoside. He interprets this result as due to an accumulation of lesions by ara C-inhibition of repair of DNA-base damage. It is base damage, in Preston's view, that initiates the production of chromosome aberrations. Natarajan and Obe (1984) attribute Preston's results to inhibition of DNA ligase by ara C.

Perhaps the greatest contribution of cytogenetics to the field of radiation biology was the discovery of mitotic death as a major mode of radiation-induced cell lethality. This brought the study of radiation effects down to the subcellular level. Despite this accomplishment, conventional mitotic chromosome studies are subject to a number of technical difficulties and inherent limitations that restrict their usefulness. The technical difficulties include 1) the dependence of aberration yield on post-irradiation sampling time, 2) a mixing of first and second mitoses due to radiation-induced cell-cycle delays, 3)

possible loss of the most severely damaged cells due to interphase death, and 4) even the best chromosome preparations may not reveal all of the aberrations present. As with the colony-formation assay, the inherent limitations of mitotic chromosome techniques stem from an inability to see the initial leions or how they change during the course of time. The challenge now is to push the study of radiation effects on cells backwards in time and to finer levels of detail.

DNA Strand Breaks vs LET

Christensen et al. (1972) conducted a LET study of breakage in ϕX174 DNA irradiated in a protective buffer with γ-rays and low-energy ion beams. They observed a LET dependence for strand breakage with RBE values >1 for double strand breaks (dsb) but not single strand breaks (ssb). Exposing V79 cells to x-rays and low-energy particle beams, Ritter et al. (1977) investigated the induction and repair of DNA strand breaks by alkaline sucrose gradient sedimentation. This method responds to ssb, dsb and alkali-labile sites. They found a continuous decline in the initial yield of strand breaks above 10 keV/μm. When maximum rejoining of strand breaks was allowed (8½ hrs incubation at 37°C) a fraction of the initial breaks failed to rejoin. The relative numbers of these non-rejoining DNA breaks plotted vs LET showed a peak in the same LET range as for cell killing. It was suggested that the non-rejoining lesion may be a dsb. Roots et al. (1979) used high energy particle beams to examine DNA breaks in T1 cells by hydroxylapatite chromatography. Their results were similar to those of Ritter et al. (1977). In both studies a maximum of ~ 20 to 25% of the initial breaks failed to rejoin at 100 keV/μm. Kraft et al. (1987) examined ssb and dsb in SV40 DNA irradiated in a low molarity Mg $Cl_2$/Tris buffer. With $^{60}Co$ γ-rays as a reference, the RBE's for either ssb or dsb were never greater than 1 and diminished with increasing LET. For all ions, a common strand-breakage

efficiency vs LET curve existed below 100 keV/μm. As the LET increased above 100 keV/μm the common curve split into separate curves for each ion with the heavier ions being more effective than the lighter ions at the same LET. The intracellular strand-breakage data of Kampf and Eichhorn (1983) and Aufderheide (1987) showed a RBE of less than one at all LET values only for ssb. For dsb a maximum RBE substantially greater than 1 was found at ~ 100 keV/μm. The discrepancy between the RBE values for dsb obtained intracellularly and in solution was explained by Kraft et al. (1987) as follows. Strand breaks can occur either by a direct transfer of energy from an incident particle to DNA, or indirectly through the attack of free radicals, mainly OH, that were created by energy transfer events in the aqueous medium surrounding DNA. For the direct effect, as the LET increases so does the probability of producing a dsb from two ssb created independently in close proximity. This mechanism allows an RBE >1. For the indirect effect, the local density of free radicals about a particle track increases with increasing LET but so does the probability of radical recombination. This weakens the effectiveness of strand breakage by the indirect pathway so that by the indirect effect alone the RBE would never be greater than 1. In a dilute aqueous milieu, both DNA strand-breakage pathways are operative but the indirect effect predominates causing an RBE <1. Radical scavanging action in the highly protective intracellular environment greatly reduces the influence of the indirect effect. In this case the direct effect is sufficiently strong to cause an RBE >1.

The analysis of DNA strand breakage and rejoining has provided valuable information about radiation damage at the molecular level. Strand break assays do, however, suffer from certain drawbacks. For example: 1) Under alkaline conditions ssb, dsb, and alkali-labile sites all contribute to the measured effect but only the dsb is thought to

participate in the formation of lethal chromosome aberrations. 2) Radiation doses well above the range of biological significance are required for most strand-break assays. 3) The distribution of lesions among the irradiated cell population cannot be determined. 4) The molecular groups at the ends of broken DNA strands are unknown. 5) Repair and misrepair are not differentiated in measurements of rejoining.

Premature Chromosome Condensation

Spontaneous cell fusion is occasionally observed under certain circumstances, such as between maturing myoblasts or between adjacent cells in a virus-infected culture. However, the potential of cell fusion as a research tool was not harnessed until 1965 through the work of Harris and Watkins. They discovered that the Sendai virus, a RNA virus known for its pathogenicity in mice, retained its ability to induce cell fusion even after having been sterilized with ultraviolet light. UV-inactivated Sendai virus was found to be a potent reagent for inducing fusion between any of a wide variety of plant and animal cells. Since that time a number of chemical agents, most notably polyethylene glycol, and also electric-field pulses have been discovered to be active inducers of cell fusion (Klebe and Mancuso, 1981; Teissie et al., 1982). The mechanism by which a fusogen creates a union between two cell plasma membranes is still unknown but is under active investigation. It has been observed that fusogens temporarily permeablize cell membranes (Bryant, 1984; Teissie et al., 1982; personal observations). This suggests that cell membrane damage and repair may be involved in the fusion process.

In 1970 Johnson and Rao performed an elegant study of cell-cycle control. Heterokaryons were formed by fusing cells in different parts of the cell cycle and then observing the influence on further cell-cycle progression of each nuclei in the hybrid. They discovered that

unidentified factors in a mitotic cell had the ability to induce condensation of interphase chromosomes. The phenomenon was called "premature chromosome condensation (PCC)" because the condensation of interphase chromosomes would be premature in a normal cell cycle. The morphology of PCC chromosomes depended on cell-cycle stage at the time of fusion. In $G_1$ each PCC chromosome was composed of a single chromatid while a $G_2$ PCC chromosome has two chromatids and resembles an elongated mitotic chromosome. S-phase PCC chromosomes are composed of thick and thin segments giving a "pulverized" appearance although further research has indicated that they are probably not broken. A number of factors have been identified that are active in either promoting or inhibiting PCC. Low pH, certain positively charged compounds (Mg, spermine, putrecine) and ATP promoted PCC while high pH, spermidine and all negatively charged compounds tested were inhibitory (Rao and Johnson, 1971; Obara et al., 1974). Evidence is accumulating that the same biological factor, or factors, are associated with the condensation of chromosomes seen in three different phenomena, namely mitosis, meiosis and PCC, and that the factor(s) are quite similar in many animal species (Sunkara et al., 1979). There is also evidence that protein phosphorylation is directly involved in the condensation process (Wu and Gerhart, 1980; Hermann et al., 1984).

Waldren and Johnson (1974) using $G_1$ HeLa cells and Hittleman and Rao (1974) using $G_2$ CHO cells were the first to use PCC as a means for investigating radiation-induced breakage and rejoining of interphase chromosomes. To distinguish them from DNA strand breaks or breaks in mitotic chromosomes, the lesions revealed by PCC are often called "interphase chromosome breaks" or more simply "chromatin breaks". In $G_1$ cells, 10 times as many chromatin breaks were seen by the PCC technique compared to what was seen when cells were irradiated in $G_1$ and scored for

breakage in mitosis. This demonstrated the PCC technique to be a sensitive indicator of chromosome damage. A linear dose response was found by Waldren and Johnson (1974). They also observed a time-dependent reduction in the number of breaks during post-irradiation incubation. The rejoining rate was similar to the rate of increase in cell survival that occurs with PLD repair. The work of Waldren and Johnson was confirmed and extended by Cornforth and Bedford (1983a,b;1985) using a plateau-phase human diploid cell line (AG1522). By comparison to the DNA dsb data of Blocher and Pohlit (1982), Cornforth and Bedford found only 15% of the dsb to be expressed as chromosome breaks and suggest that the other 85% of dsb may be located in heterochromatin which might prevent the separation of broken ends. The work of Pantelias (1986) lends support to this hypothesis. No breakage was seen in fully-condensed x-irradiated mitotic chromosomes. Apparently the compact structure of a condensed mitotic chromosome prevented the expression of dsb as chromosome breaks. Alternatively, it is possible that a fast-rejoining fraction of dsb is missed by the PCC assay. As with DNA strand breaks, not all interphase chromosome breaks rejoin even after long incubation periods. Normal human cells (AG1522 and AG6234) rejoined all but ~ 5% of their initial chromosome breaks while radiosensitive ataxia telangiectasia cells (AT5BI and GM2052) failed to rejoin 5 times as many (27%) of their initial breaks (Cornforth and Bedford, 1985). The yield of initial breaks per unit dose was the same in each cell line. In each cell line, the rejoining fraction of breaks followed first order kinetics with similar half-times. After a 24 hour post-irradiation incubation period, the residual number of PCC fragments, which are the result of unrejoined breaks plus ring chromosome aberrations, closely approached the number of chromosome aberrations observed in mitosis (Cornforth and Bedford, 1987). All of these findings taken together led Cornforth and

Bedford (1987) and Bedford and Cornforth (1987) to propose that the increase in survival seen in either delayed-plating or dose-fractionation experiments could be quantitatively explained on the basis of interphase chromosome breakage and rejoining. Iliakis et al. (1988) investigated the effects of β-arabinofuranosyladenine (araA), a DNA polymerase inhibitor, on both PLD repair and chromosome break rejoining in x-irradiated, plateau-phase CHO cells. With increasing concentrations of araA there was a progressive loss of the shoulder in x-ray survival curves. AraA had a similar inhibitory effect on the rejoining of chromosome breaks. These results were interpreted as implying that PLD repair has a counterpart at the chromosomal level. In addition, a requirement for DNA polymerization during the course of chromosome repair was established. This finding is in agreement with that of Das and Alfert (1961) who observed increased DNA synthesis in onion root tip cells in response to x-irradiation, which may have been due to the stimulation of DNA repair.

Because they lack a clearly defined centromere, it has been difficult to detect aberrations in $G_1$-phase PCC chromosomes; an important exception being the ring chromosomal aberration. Pantelias and Maille (1985) determined the yield of ring PCC chromosomes in $G_o$ human lymphocytes exposed to x-rays along with the yield and rejoining kinetics of chromatin breaks. They found that the dose response for ring aberrations scored 24 hours post irradiation could be fitted to a linear-quadratic expression. The same study also revealed that a very different time course was followed for the ring aberration yield as compared to the rejoining of chromatin breaks. Although they observed a rapid decline in chromatin breaks during the first 3 hours following irradiation, the yield of ring aberrations did not rise significantly until more than 3 hours had elapsed. The frequency of rings per cell in

the irradiated cell population followed a Poisson distribution while chromosome fragments were overdispersed. Edwards et al. (1979) reached a similar conclusion for the distribution of chromosome aberrations scored in mitosis.

Bedford and Goodhead (1987) irradiated noncycling $G_1$ human H19 cells with $^{238}Pu$ α-particles (LET = 130 keV/μm). They found a linear dose response and an RBE of ~ 2 for initial chromatin breakage. Xian-Li and Ngo (1988) irradiated $G_1$-phase V79 cells with γ-rays and fast neutrons. Both radiations induced a linear dose response for chromatin breakage. An RBE = 2.4 was observed.

It might be expected that more breaks would be found in $G_2$ than in $G_1$ after equivalent doses because of the greater DNA content of each cell. However, four to five-fold fewer breaks per unit dose were observed in cells irradiated with x-rays and analyzed in $G_2$ (Hittleman and Rao, 1974; Hittleman and Pollard, 1982). Hittleman and Pollard (1982) made a comparison between the repair kinetics of $G_2$ interphase chromosome breaks as assayed by PCC and the repair kinetics of DNA strand breaks as measured by alkaline and neutral elution techniques. No rejoining of chromosome breaks was observed during the first 30 minutes following irradiation. In the next 30 minutes nearly half of the original breaks rejoined. Asymmetrical exchange-type aberrations are easily scored in $G_2$ PCC. All of the exchange aberrations appeared to have already been formed by the earliest time point observable with PCC. Cycloheximide completely inhibited the rejoining of chromosome breaks but had no effect on the number of exchanges. Based on these results the authors suggest that there is no connection between rejoining of breaks measured by PCC and the formation of exchange aberrations. The interpretation of these observations may be complicated by cycling of cells into and out of the $G_2$ compartment during the course of the

incubation period. The same study found no correlation between the kinetics of chromosome break rejoining and DNA strand break rejoining measured under either alkaline or neutral conditions. Cycloheximide, which strongly inhibited the rejoining of chromosome breaks, had no effect on the rejoining of DNA breaks. Hittleman and Pollard suggest that only a fraction of DNA strand breaks may be involved in visible chromosome damage and that chromosome repair may require more than simply rejoining the breaks in DNA. Hieber and Lucke-Huhle (1983) exposed V79 cells to α-particles from an $^{241}Am$ source. The LET of this radiation at the position of the cells was ~ 120 keV/μm. Using the PCC technique to assay chromosome damage in $G_2$ cells they observed gaps and breaks in chromatids similar to those seen after x-irradiation (Hittleman and Pollard, 1982). In addition they observed a more severe lesion that appeared to be a long stretch of decondensed chromatin within a chromatid. A multiplicity of breaks per chromosome was suggested as a cause for the localized failure of chromosome condensation.

The studies reviewed here demonstrate the usefulness of the PCC technique's ability to visualize chromosome breakage in interphase cells at a time when repair processes are still at work. The chromosomal damage hypothesis of cell lethality has been strengthened by these studies. Yet the PCC technique also has its weaknesses, two of which are: 1) The time interval from irradiation of a sample, through chromosome condensation, until final fixation, is inaccessible to observation. Thus one cannot see the initial radiation-induced lesions or whatever early modification they might undergo. In this context, it should be remembered that the phrase "initial chromatin breaks" refers to initially observed, not initially produced. In the discussion of ring PCC chromosome formation, a quantitative estimate will be made of the amount of repair that takes place during the PCC process itself. 2)

Chromosomal damage in the S phase of the cell cycle cannot be investigated by the PCC technique because of the pulverized appearance of PCC chromosomes undergoing DNA synthesis.

# MATERIALS AND METHODS

## Cell Lines and Growth Conditions

Three cell lines were used during the course of the research reported here. The CHO-SC1 cell line, isolated by Dr. L. Thompson of Lawrence Livermore Laboratory from a clone of the original CHO cell line started by Puck et al. (1958), was used as a source of mitotic cells. A second cell line, also isolated by Dr. Thompson following mutagenesis of CHO-SC1 cells and designated as CHO-tsH1 by him, was used as the test cell in most of the thesis work (Thompson et al., 1973). This cell line has a defect in its leucyl-transfer-RNA synthetase that causes a shut-down of most protein synthesis at elevated temperatures. This property of the CHO-tsH1 cell was not used in any of the thesis experiments. In the later part of the thesis work, investigations of chromosomal misrepair required the use of a human/hamster hybrid cell line. Isolated by Dr. R. Athwal of the New Jersey Medical School and designated UV24C2-3, the hybrid cell line contains a single copy of the human #2 chromosome that accounts for ~ 4% of total cellular DNA. Integration of a dominant selectable marker, the *E. coli* xanthine-guanine phosphoribosyltransferase (Ecogpt) gene, into the human chromosome maintains karyotypic stability of this hybrid cell line (Athwal et al., 1985) when cells are grown in a special medium. This medium contains mycophenolic acid to block purine biosynthesis and xanthine, which can be used only by those cells having an Ecogpt gene in a salvage pathway of purine synthesis. The UV24C2-3 cell line was also provided to us by Dr. Thompson.

The CHO-tsH1 cell line was maintained in exponential growth by twice-weekly transfers. Incubations were at 35° in a 5% $CO_2$ atmosphere. Under these conditions cultures had a doubling time of ~ 16 hours that remained nearly constant throughout the course of the thesis work. Fresh

cultures were started from frozen stock at about 6 month intervals. The UV24C2-3 cells were occasionally passaged in "MAXTA" selection medium. Doubling times were 16 hours in growth medium and 33 hours in MAXTA medium. Growth and selection media are fully described in the Appendix. In preparation for the experiments, cells of either type were suspended in growth medium at $1.25 \times 10^6$/ml and seeded into 35 mm plastic dishes (Falcon #3001) at 2 ml/dish. Twenty-four hours later the growth medium was replaced by medium prepared without serum. After an additional 24 to 36 hours the cultures were ready for experimentation. This treatment results in an enriched population of $G_1$ cells.

Radiation Exposures

X-ray exposures were done using a Philips cabinet irradiator, model Norelco, Mg 150. The machine was operated at 150 kVp and 12.5 mA. The beam was filtered with 1.02 mm Al and 0.5 mm Cu. Under these conditions the half value layer was 1.3 mm Cu + 1.0 mm Al. Dosimetry was performed at the start of each experiment using a Victoreen condenser R-meter. A source-to-sample distance of 10 inches was used in all experiments with the cell monolayers placed perpendicularly to the direction of incidence of the beam. This configuration resulted in a dose rate of ~ 120 rad/min with a center-to-edge variation in dose of < 8%. The LET of the x-ray exposures is estimated to be in the 1.5 to 3.5 keV/μm range (Johns and Cunningham, 1974; Barendsen et al., 1963; Amols et al., 1986).

Particle beam exposures were performed at the Bevalac, a synchrocyclotron located at Lawrence Berkeley Laboratory and operated under the auspices of the Department of Energy. The Bevalac, which was created in 1974 by using the SuperHILAC (a linear accelerator) to inject accelerated charged particles into the Bevatron (a synchrotron), can produce relativistic beams of ions as light as protons or as heavy as

uranium. Such beams have an intensity and range that make them suitable for clinical radiotherapy trials.

Irradiation of cell monolayers was performed in the track segment mode, i.e., with the plane defined by the monolayer placed perpendicular to the incident beam so that the particles passed through the bottom of the plastic petri dish. To ensure 5% dose uniformity over the irradiated sample, lead scattering foils were placed in the beam line. Dosimetry was accomplished by placing a parallel plate ionization chamber in the beam line just before the sample. Prior to each experiment, the ionization chamber was calibrated against a tissue-equivalent dosimeter (EGG model No. IC-17A) placed at the sample position. For the two higher LET neon experiments a variable thickness water column was used to place the Bragg peak closer to the sample position (Fig. 1). The higher LET neon beams also required dose correction factors of 1.06 and 1.18, respectively, for the 100 keV/μm and 183 keV/μm exposures (Ngo et al., 1981) to account for additional slowing of the particles as they passed through the bottom of the petri dish. All other particle beam exposures were done in the plateau of the Bragg curve. A detailed description of Bevalac operating principles, the physical characteristics of Bevalac beams and irradiation procedures can be found in one of the following references: Blakely et al. (1979; 1984), the Bevalac Users Handbook, and Pirruccello and Tobias (1980). Table 1 shows the most important physical characteristics of the 9 particle beams used in this work.

Cell Survival

Cell survival was determined by the colony-formation assay of Puck and Marcus (1956). Following graded doses of radiation, cell cultures were either trypsinized (.05% trypsin + 0.2% EDTA, Gibco) immediately or, where appropriate, after a repair incubation period at 35°C (CHO-tsHI cells) or 37°C (UV24C2-3 cells). Enough cells were seeded into 5 ml of

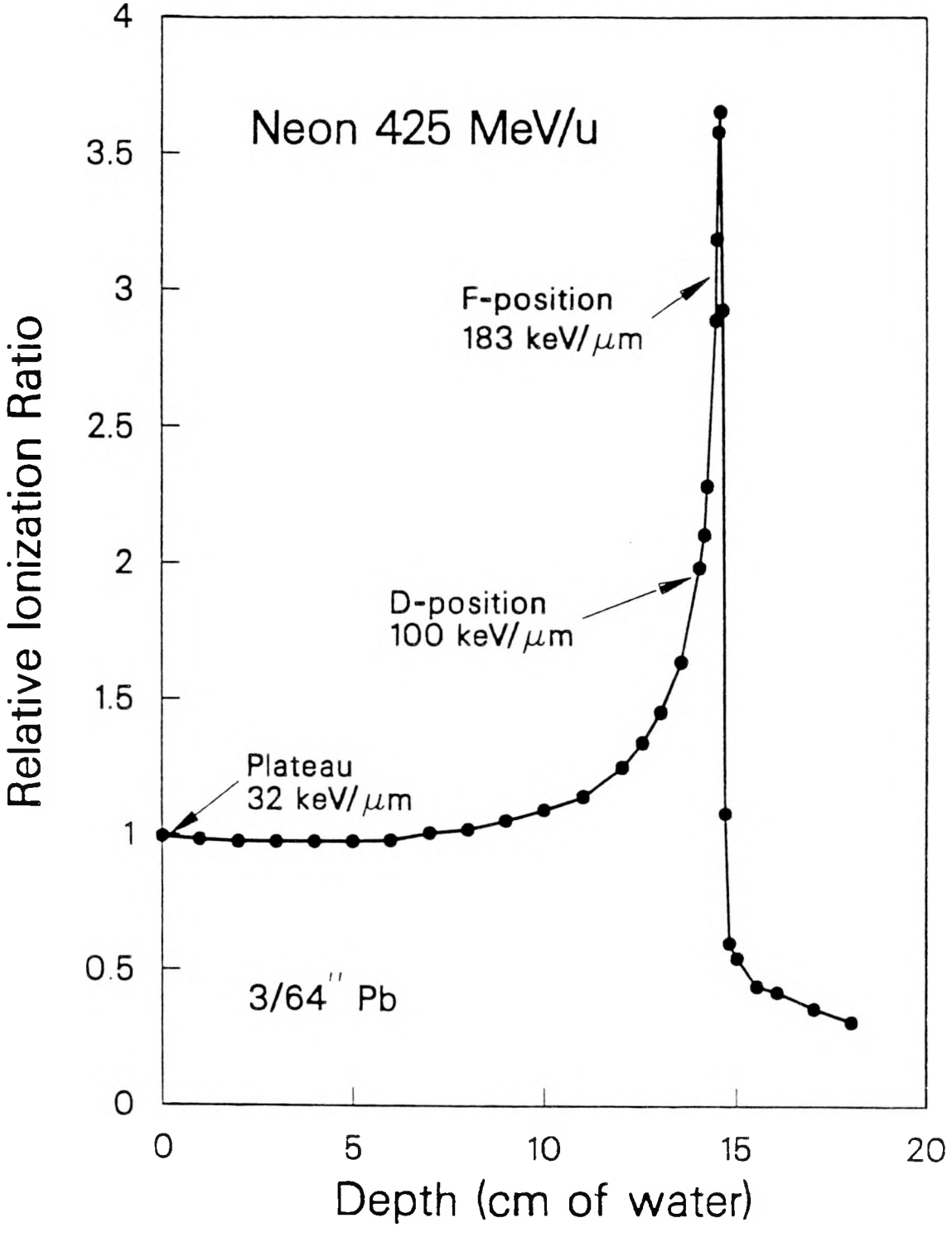


XCG 874-6877 A

Figure 1. Bragg curve for the 425 MeV/amu neon beam. Biological samples were placed at one of the three positions indicated by arrows.

TABLE 1

PARTICLE BEAM DATA

| Ion | Mass (amu) | Charge[a] | Initial Energy (Mev/amu) | LET (keV/μm[b]) | Energy at Sample Position[c] (MeV/amu) |
|---|---|---|---|---|---|
| H | 1 | +1 | 150 | 0.562 | 150 |
| C | 12 | +6 | 300 | 13.74 | 258 |
| Ne | 20 | +10 | 425 | 32 | 360 |
| Ne | 20 | +10 | 425 | 100 | 65.3 |
| Ar | 40 | +18 | 400 | 115 | 290 |
| Ne | 20 | +10 | 425 | 183 | 31 |
| Nb | 93 | +41 | 600 | 475 | 400 |
| U | 238 | +68 | 960 | 1900 | 864 |
| U | 238 | +68 | 325 | 2700 | 300 |

a. acceleration charge
b. dose-averaged $LET_{\infty}$ as estimated by Lawrence Berkeley Laboratory staff scientists
c. estimated from tables in the "Bevalac User's Handbook", Lawrence Berkeley Laboratory Biology and Medicine Publication 101, 1977

Tabulated here are the physical characteristics of the 9 particle beams used in the thesis work.

growth medium in 25 $cm^2$ Falcon flasks to yield an anticipated 150 to 180 colonies per flask. For the dose-response curves, 8 flasks were plated for each of 2 zero-dose controls for the highest dose point. Four flasks were plated for each of the intermediate survival points. For the PLD repair curves, 8 flasks were plated for each of 2 zero-dose controls as well as all time points. After 10 days the medium was emptied from the flasks and colonies were stained with either 0.1% crystal violet in 25% ethanol (CHO-tsH1 cells) or 1% methylene blue in 30% ethanol (UV24C2-3 cells). Each colony containing 50 or more cells was judged to have arisen from a viable cell. Plating efficiency was typically in the range of 80 to 100%. The surviving fraction was calculated by dividing the ratio of the average number of colonies per flask to the average number of cells seeded per flask by the plating efficiency. A linear-quadratic curve was fit to dose-survival data using a computer program designed by Dr. Norman Albright (Rad. Res. 112, 1987; LBL Publication 22347, 1988). This same program was used for RBE determinations.

Collection of Mitotic Cells

The PCC technique requires the ready availability of large numbers of mitotic cells. Furthermore, the differential staining procedure of Cornforth and Bedford (1983a) which will be described later, requires that the mitotic cells have chromosomes that are fully substituted with bromodeoxyuridine (Brd Urd). The collection process described here is based on the observation that mitotic cells are more loosely attached than interphase cells and can be selectively dislodged from the cell monolayer by reciprocal shaking (Terasima and Tolmach, 1961). Mitotic cells are collected from CHO-SC1 cell cultures that have been growing continuously in the presence of $6 \times 10^{-7}$ molar Brd Urd for several months. It is convenient to keep samples of Brd Urd-substituted CHO-SC1 cells frozen in liquid $N_2$. About 1 week prior to a mitotic cell

collection, a sample is thawed and the cells are allowed to grow at 37°C in medium + Brd Urd.

24 hours prior to beginning a mitotic cell collection, 15-75 $cm^2$ flasks (Falcon #3024) are seeded with 4.5 x $10^6$ cells in growth medium + 6 x $10^{-7}$ M Brd Urd + 17 mM Hepes buffer. The flasks are transferred to a 37°C warm room shortly before starting the collection procedure. The collection procedure starts with 3 "clean-up" shakes to remove dead cells and debris and 3 additional shakes with 2 µg/ml colchicine added to the medium. Each shake is separated by 20 minutes. Two mitotic cell harvest shakes follow 3½ hour collection intervals. In the context used here, "shake" is defined as a 1 minute episode of shaking on an Eberbach Corp. reciprocating table set for a 2 inch stroke length and a frequency of 118 cycles per minute. The medium used during the collection intervals contains 2 µg/ml colchicine plus 17 mM Pipes buffer instead of Hepes. Mitotic cells are centrifuged to a pellet and then resuspended in growth medium + 15% fetal calf serum + 17 mM Pipes + 2 µg/ml colchicine + 4% DMSO. The cells are then put into freezing vials (Nunc), frozen by lowering the temperature at a controlled rate in a Union Carbide biological freezer, and stored in liquid nitrogen. Mitotic cells collected in this way are designated as CHO-MB.

Premature Chromosome Condensation

The operational complexity of the Bevalac, especially with the acceleration of exotic ion species, coupled to the competing demands of many investigators often required that changes be made in the experimental protocol, sometimes on short notice. To allow for this, an extra degree of flexibility had to be built into the PCC procedure. The method described here follows that of Pantelias and Maille (1983) with modifiations. The procedure is shown schematically in Figure 2. Recipes

Methods:

A. The System

1. Confluent serum-deprived CHO-tsH1 cells

2. Track segment exposures

B. Premature Chromosome Condensation (PCC) Method

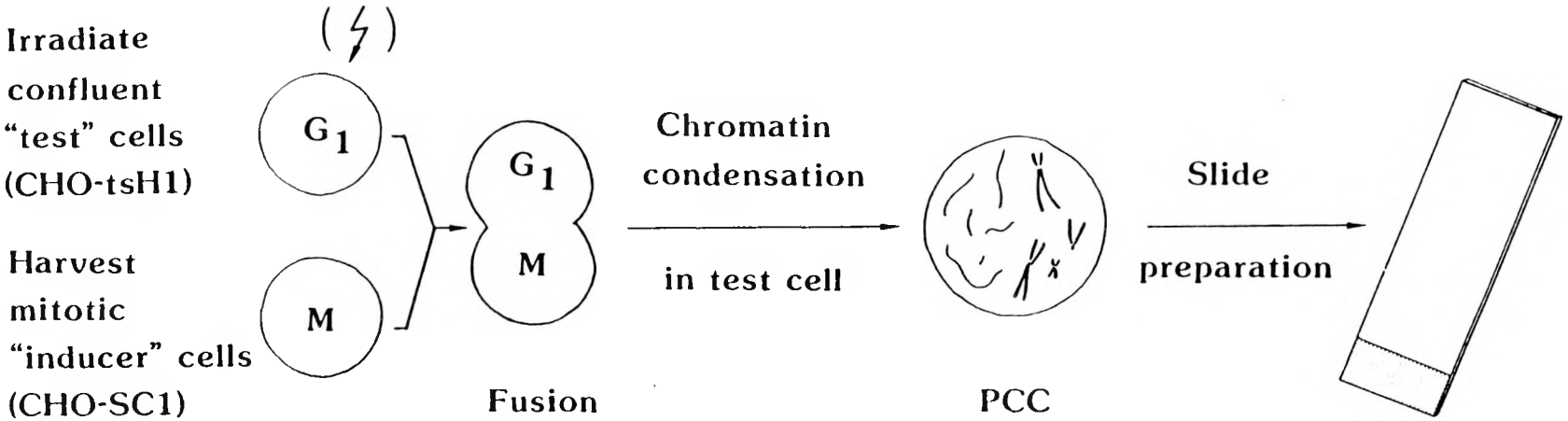


Figure 2. The PCC method. Shown here is the sequence of steps followed in the PCC technique.

for the solutions used in the PCC procedure will be found in the Appendix.

Remove vials of frozen mitotic CHO-MB cells from a liquid $N_2$ dewar. Usually from 3 to 4 x $10^6$ mitotic cells are needed for each fusion. Thaw the vials. Transfer the contents to a 15 ml centrifuge tube and add 1.5 ml of thawing medium for each vial. Put the cells on ice until needed. While it is best to thaw mitotic cells as close to the time of fusion as possible, good results can still be obtained for several hours after thawing as long as the cells are kept on ice. The stockpiling of frozen CHO-MB effectively uncouples the collection of mitotic cells from the rest of the PCC protocol. CHO-MB stored in liquid $N_2$ for 2 years have successfully induced PCC.

Aspirate the medium from the irradiated dishes. Wash twice with cold medium prepared without fetal bovine serum. Trypsinize the cultures using trypsin plus 25 µg/ml cycloheximide for 5 minutes at 37°C or until cells detach. Add 1 ml of cold PCC medium and transfer cells to a 15 ml centrifuge tube. Pipette the cells repeatedly to form a single cell suspension. Add mitotic cells (3 to 4 x $10^6$ per fusion). Pellet the cells by centrifuging for 4 minutes on setting #4 of an ICU clinical centrifuge. Remove the supernatant by aspiration. Resuspend the cells in 1.5 ml of cold wash solution and transfer to a 16 mm round bottom test tube (Falcon #3033). The use of a conical bottom centrifuge tube at this point will not give satisfactory results. Centrifuge for 3 minutes on setting #4. Aspirate most of the supernatant then carefully invert the test tube to drain off the remaining liquid. Let the tube remain inverted for 1-2 minutes. Blot or aspirate any drops that run down the side of the test tube. This step prevents dilution of the fusogen by allowing the pellet to drain completely.

Draw ¼ ml of warm (37°C)polyethylene glycol (PEG)/Hepes solution into a 1 ml hypodermic syringe fitted with a 1 inch 20 gauge needle. The PEG/Hepes solution can be prepared in advance and stored in 2 ml freezing vials at -20°C. Turn the test tube upright, insert the syringe and eject the PEG/Hepes onto the cell pellet. Remove the syringe. For the next 60 seconds shake the test tube gently with just enough motion to break up the cell pellet. For the fusion process to be successful, the cell pellet must break up into small clumps of a few cells each. Too much shaking will turn the pellet into a single-cell suspension. This reduces effectiveness since cells which do not touch cannot fuse. Next, the PEG/Hepes is diluted slowly by adding 2.5 ml of wash solution drop-by-drop over a 2 to 3 minute interval. Since the fusogen is hypertonic, the slow dilution is necessary to prevent the rupture of weakened cell membranes by osmotic shock. Add 2.5 ml of thawing medium. Pellet the cells, aspirate the supernatant and drain completely. Add 2 ml of PCC medium, cap the test tube and place it into a 37°C water bath. After 10 minutes add 2 ml of PCC medium/Pipes. The lower pH of the medium buffered with Pipes promotes chromosome condensation (Obara et al, 1973 and 1974). Allow the test tube to remain in the water bath for an additional 35 minutes. The cells are now ready for microscope slide preparation.

Microscope Slide Preparation

Compared to ordinary mitotic chromosome squashes, the preparation of high quality microscope slides with cells from a PCC experiment was found to be more difficult yet more critical to the ease and accuracy of scoring. The methods described here have evolved over several years and give good results in most cases.

Following fusion and premature chromosome condensation, cells are resuspended in hypotonic KCl (75 mM) for 11 minutes. Colcemid (0.2

µg/ml) was often added during hypotonic treatment but may not be necessary. After pelleting, all but ½ ml of supernatant is removed and the cells are resuspended in this volume. As a fixative, 95% ethanol and glacial acetic acid are used in the ratio of 3:1. With constant agitation of the cell suspension 7 ml of fixative is added using a Pasteur pipette (Fisher #13-678-6A) fitted with a rubber bulb. The rate at which fixative is added is important; too fast and cells lyse, too slow and fixation is poor. A workable compromise is to add the first 2 ml of fixative at a rate that produces a series of fast drops, almost a stream, from the pipette. This rate is faster than recommended in many published protocols, but experience shows it to produce better results. The remainder of the 7 ml can be added faster. Cells are often trapped in a stagnant bottom layer with nearly pure fixative above. Use the dropping pipette to mix the contents of the centrifuge tube. Fixation is completed after 20 to 30 minutes at room temperature. Wash cells 3 times in fixative (methanol/acetic acid, 3:1). After the last wash, cells are resuspended in ~ 0.3 ml of fixative.

It is necessary to clean microscope slides before using them (the so-called "precleaned" slides are never clean enough). Best results were obtained with the commercial glassware cleaner "No Chromix" dissolved in sulfuric acid. Slides are immersed in the mixture for 15 to 20 minutes and then thoroughly rinsed in distilled water (not tap water!). To make a cell spread, fog a clean dry slide by breathing on it, then allow a single drop of cell suspension to fall onto the slide from a height of ~ 6 inches. Blow on the slide to spread the drop. Let the slide dry. At this point the slide is evaluated under phase contrast (400X). Ideally, cells should show good spreading between chromosomes, thin cytoplasm and good chromosome morphology. Poor results are usually of two types; underspreading (clumped chromosomes and thick cytoplasm) and

overspreading (cell lysis with scattered chromosomes). The degree to which chromosomes spread seems to be related to the time it takes the fixative to dry, with a longer drying time leading to increased spreading. Low heat, fanning a slide or using less acetic acid in the last wash step will decrease drying time. For the two cell lines used in the thesis work, resuspension in a 5:1 mixture of methanol and acetic acid prior to dropping, and allowing the slide to dry without further manipulation after dropping, usually produced very good cell spreading.

Differential Staining

The procedure described here is a modification of the method developed by Cornforth and Bedford (1983a) which, in turn, is based on the Fluorescence-plus-Giemsa method used by Perry and Wolff (1974) to detect sister chromatid exchanges. Differential staining causes PCC fragments from the test cells to stain darkly while mitotic chromosomes from the inducer cells stain lightly. Thus one can easily distinguish small telocentric mitotic chromosomes from PCC fragments. In addition, since the mitotic index is always less than 100%, one can distinguish, and avoid scoring, occasional heterokaryons resulting from the fusion of a mitotic cell to a contaminating interphase cell. The advantage of differential staining is that it can significantly improve the accuracy of scoring.

Slides that are between 1 day and 2 weeks old are stained for 15 minutes in the fluorescent dye Hoechst No. 33258 (5 µg/ml in Sorensen's buffer, pH 6.8). Rinse twice and allow to dry. Put one drop of Sorensen's buffer, pH 6.8 onto a slide then place a 22 x 40 mm #1 coverslip onto the slide. Place 1 to 5 slides onto a 57°C hotplate. Temperature is measured with a thermometer placed on the hotplate so that its bulb is in contact with the heating surface. A 15 watt long wave ultraviolet light bulb is lowered to a distance of 2 cm above the

hotplate. After a 5 minute UV exposure, slides are removed from the hotplate and put into a Coplin jar containing distilled water. The coverslips will easily slip off after about a minute. Slides are rinsed once then allowed to dry. The temperature of the hotplate and length of the UV exposure may have to be adjusted to achieve best results. This procedure has the added benefit of improving staining by removing much of the cytoplasm from cell spreads. Final staining is done with a 4% Giemsa (Gurr's improved R66) solution in Sorensen's buffer, pH 6.8 for 16 minutes. Slides are rinsed 3 times with distilled water then allowed to dry.

Fluorescense In Situ Hybridization

The methods used here are those of Pinkel et al. (1986). The DNA in chromosome spreads was denatured by immersing a microscope slide into a 70°C solution of 70% formamide, 2 x SSC (see Appendix) for 2 minutes. A probe consisting of human genomic DNA (Sigma) biotinylated by nick-translation (BRL) was also denatured. The stringency of the hybridization ensured that the probe bound only to the human chromosome in the UV24C2-3 cells. Staining with fluorescein conjugated to avidin renders the human chromosome fluorescent. The fluorescent signal is often weak at this point, but can be amplified ~6 fold by successive application of biotinylated anti-avidin antibody followed by a second round of staining with fluoresceinated avidin. Total DNA is counterstained with propidium iodide. Fragments of the human chromosome fluoresce a bright yellow in contrast to the red fluorescence of hamster chromatin. Some degradation in chromosome morphology appears to be the inevitable result of the harsh denaturation procedure.

Scoring a PCC Experiment

Scoring a PCC experiment is accomplished with the use of a light microscope equipped with a 100x high numerical aperature oil immersion

objective and a drawing tube apparatus. To score, one simply counts the number of $G_1$-PCC fragments in 20 or more cell spreads. However, counting is not a trivial matter. Three sources of difficulty can be identified. First, when scoring a cell with numerous fragments it is easy to lose track of which fragments have been counted and which still remain to be counted. The drawing tube apparatus, which is in essence a camera lucida, provides an effective solution to this problem. With it, the image of a blank piece of white paper is superimposed onto the image of a cell spread. As it is counted, each fragment is "crossed off" by placing a mark on the white paper at the appropriate position. The second source of difficulty arises from the mitotic cell population used in the PCC procedure. Mitotic chromosomes occasionally overlap PCC fragments and small telocentric chromosomes may be mistaken for PCC fragments. Also, some interphase cells contaminate the mitotic inducer cell population (the mitotic index is never 100%). Contaminating interphase cells can fuse to mitotics and give rise to cell spreads that may be mistaken for fusions between inducer and test cells. These problems are minimized by the differential staining method of Cornforth and Bedford (1983a). With this method, PCC fragments are made to stain darker, and a somewhat different color, than either mitotic chromosomes or PCC fragments created by fusions of mitotics to interphase cells contaminating the inducer cell population. Because they provide effective technical solutions to the problems encountered, the use of a drawing tube and the differential staining procedure greatly enhance the accuracy of scoring a PCC experiment. A third problem that arises is not as easily solved. The centromeres of both mitotic and PCC chromosomes occasionally remain unstained by Giemsa. This is seldom a problem when counting mitotic chromosomes because of their bivalent structure. However, a nonstaining region in a monovalent PCC chromosome can be interpreted two ways; as due

to the presence of a centromere or as due to the coincidental alignment of two separate PCC fragments. The final count will depend on the particular interpretation chosen in such cases of ambivalence. One approach to resolving this problem is to score the zero dose controls first. It is expected that most unirradiated cells possess a number of PCC fragments equal to the modal chromosome number of that cell line. This expectation is used to calibrate the process of scoring. One learns to associate gaps of a certain size with nonstaining centromeres and then continues to apply the same criterion when scoring all higher dose points. In well-spread cells, the coincidental alignment of two fragments mimicking a nonstaining centromere is likely to be an infrequent occurrence. In addition to centromeres, gaps can appear in PCC chromosomes for two other reasons. Differential staining has a tendency to produce some banding in mitotic and PCC chromosomes. In a monovalent $G_1$-PCC chromosome a light band appears as a gap. Radiation is also known to produce achromatic lesions in the chromatids of mitotic chromosomes and appears to have the same effect on PCC chromosomes. The nature of the radiation-induced gap remains unsettled (Hittleman and Rao, 1974) and no attempt was made to quantitate this lesion in the experiments reported here. In the course of experimentation with the PCC technique it was observed that variations in slide preparation and staining procedure could enhance or diminish the appearance of gaps, but never eliminate them. For the purpose of scoring, gaps are treated in the same manner as unstained centromeres, i.e., continuity of the chromatid through the gap is assumed.

For each dose or time point in the experiments reported here, from 20 to 140 PCC cell spreads on from 2 to 8 microscope slides were scored for the number of PCC fragments. The average number of PCC fragments per cell was calculated from the raw data. Each break in a chromatin fiber

increases the number of PCC fragments by one. For the purpose of data analysis, the number of chromatin breaks was defined as the number of PCC fragments minus the modal chromosome number of the cell line under study. It should be emphasized that chromatin breaks are not actually visualized in the PCC technique, rather, their number is ascertained from the counting of fragments. The standard error of the mean was used to determine error bars on the data points.

Cross sectional Area of the Cell Nucleus

A confluent serum-deprived CHO-tsH1 cell culture prepared as described earlier was rinsed once in medium without serum and then fixed with a 1:1 mixture of 95% ETOH and glacial acetic acid for 30 minutes. The fixative was removed and the dishes were allowed to dry. Cell nuclei were stained for 20 minutes in a solution of 8% Giemsa in Sorensen's buffer, pH 6.8. After rinsing in distilled water, dishes were once again allowed to dry.

Cell nuclei have an elliptical appearance when observed under a microscope equipped with a 100X oil immersion lens. Using the drawing tube apparatus, the maximum extent of the long and short axes of 20 nuclei were measured with a ruler and recorded. A conversion factor is needed to change the measured values to true dimensions. This factor was determined by using a stage micrometer to find the number of micrometers to each millimeter of measured length. The area was computed by assuming the nuclear cross section to be an ellipse.

# RESULTS

## Cell Line Characteristics

For the PCC technique, it is desirable to use a cell line having three properties: (1) few chromosomes per cell, (2) a distribution of chromosomes per cell that is narrowly peaked about the modal chromosome number, and (3) strong contact inhibition of growth. The first property increases the accuracy of scoring a PCC experiment and reduces the amount of time spent on scoring each cell. The second property reduces the total number of cells that need to be scored to reach a certain level of precision in an estimate of the average number of chromatin breaks per cell. The third property, good contact inhibition, prevents cells from cycling into or out of the $G_1$ phase of the cell cycle during repair incubations.

The CHO-tsH1 cell line has a modal chromosome number of 21, which is low in comparison to most other mammalian cell lines. 86% of the cells have 21 chromosomes while the other 14% are equally divided between those with either 20 or 22 chromosomes. This distribution also compares favorably with other cell lines. In contrast, contact inhibition of growth is poor. CHO-tsH1 cells have a tendency to grow to high cell densities in culture, exhaust nutrients in their growth medium and die off without reaching a true plateau phase. A number of experiments were performed in an attempt to force cycling CHO-tsH1 cells into a $G_0$ state without compromising their viability. The most successful results were obtained by seeding the cells at high density ($2.5 \times 10^6$ per 35 mm dish) in growth medium. 24 hours later the growth medium is replaced by medium prepared without fetal bovine serum. After an additional 24 to 36 hours cell cultures were ready for experimentation. This treatment created a confluent monolayer culture with ~ $3.5 \times 10^6$ cells per dish. Cell counts indicated no appreciable change in cell number within the 15 to 45 hour

post medium replacement interval. The mitotic index remained nearly constant throughout the plateau phase at a value approximately equal to 23% of that of exponentially growing cells. For at least two days after an experiment unused cell cultures remained viable, although there was a drop in cell number concomitant with an increase in individual cell volume at the longer observation points. The plating efficiency of confluent, serum-deprived CHO-tsH1 cell cultures was typically in the range of 80 to 100% and the x-ray survival dose response was similar to that obtained by Yezzi (1985) for exponentially growing CHO-tsH1 cells.

The UV24C2-3 cell line also has comparatively few chromosomes per cell and has a modal chromosome number of 22. In situ hybridization with a human genomic probe allows easy identification of the single human #2 chromosome in this cell line. It was discovered that there was a tendency to lose the human chromosome unless strong selective pressure was maintained. The primary use of UV24C2-3 cells was to investigate the breakage and rejoining of the single human chromosome. The loss of this chromosome in a small fraction of the cell population could be tolerated since PCC spreads without the chromosome were easily detected and not scored. An analysis of mitotic cells showed that of those cells retaining the human chromosome, 84% were pseudodiploid and contained a single copy, 14% were pseudotetraploid and had two copies, and less than 2% were pseudodiploid with two copies. Pseudotetraploid interphase cells rarely undergo premature chromosome condensation when fused to a single mitotic cell an, where PCC does occur, often from fusion to two mitotic cells, it can be easily distinguished by the excess quantity of PCC fragments present. Therefore it is the pseudodiploids with two human chromosomes that have the greatest adverse effect on scoring and their numbers are low enough to not be a serious problem.

Experiments with CHO-tsH1 Cells

A. Survival

Using a clonogenic assay, survival curves were determined for confluent, serum-deprived CHO-tsH1 cells exposed to graded doses of x-rays and 4 particle beams of different LET. The survival curves are shown in Figure 3. Table 2 shows the survival curve parameters and $RBE_{10}$ values. As has been observed by others, the $RBE_{10}$ reaches a maximum in the 100-200 keV/μm range (also, see Figure 19). A more precise estimate of the LET of maximum effectiveness could not be made based on available survival data. With increasing LET, the shoulder of survival curves was progressively reduced.

PLD repair curves were determined after exposure to x-rays or neon ions. The results are shown in Figure 4. X-irradiated CHO-tsH1 cells showed about a 2.5-fold increase in survival during a 6 hr repair period. Ne-irradiated cells showed far less recovery.

B. Chromatin Breakage, Initial Yield

The PCC technique was used to determine the initial yield of chromatin breaks in CHO-tsH1 cells exposed to x-rays and 9 particle beams. For all measurements of initial breakage, cell cultures were treated with cycloheximide starting 15 minutes before irradiation and continuing throughout the PCC process to inhibit protein synthesis. Cycloheximide was shown to decrease the rate of rejoining of chromatin breaks and to increase the time required for maximum PLD repair (Fig. 5). This finding differs somewhat from that of Wolff (1972) and Hittleman and Pollard (1982) who saw a complete suppression of chromosomal repair in the presence of cycloheximide. The question of whether cycloheximide might itself induce chromatin breakage was answered by performing a PCC analysis two unirradiated cell samples, one of which was exposed to

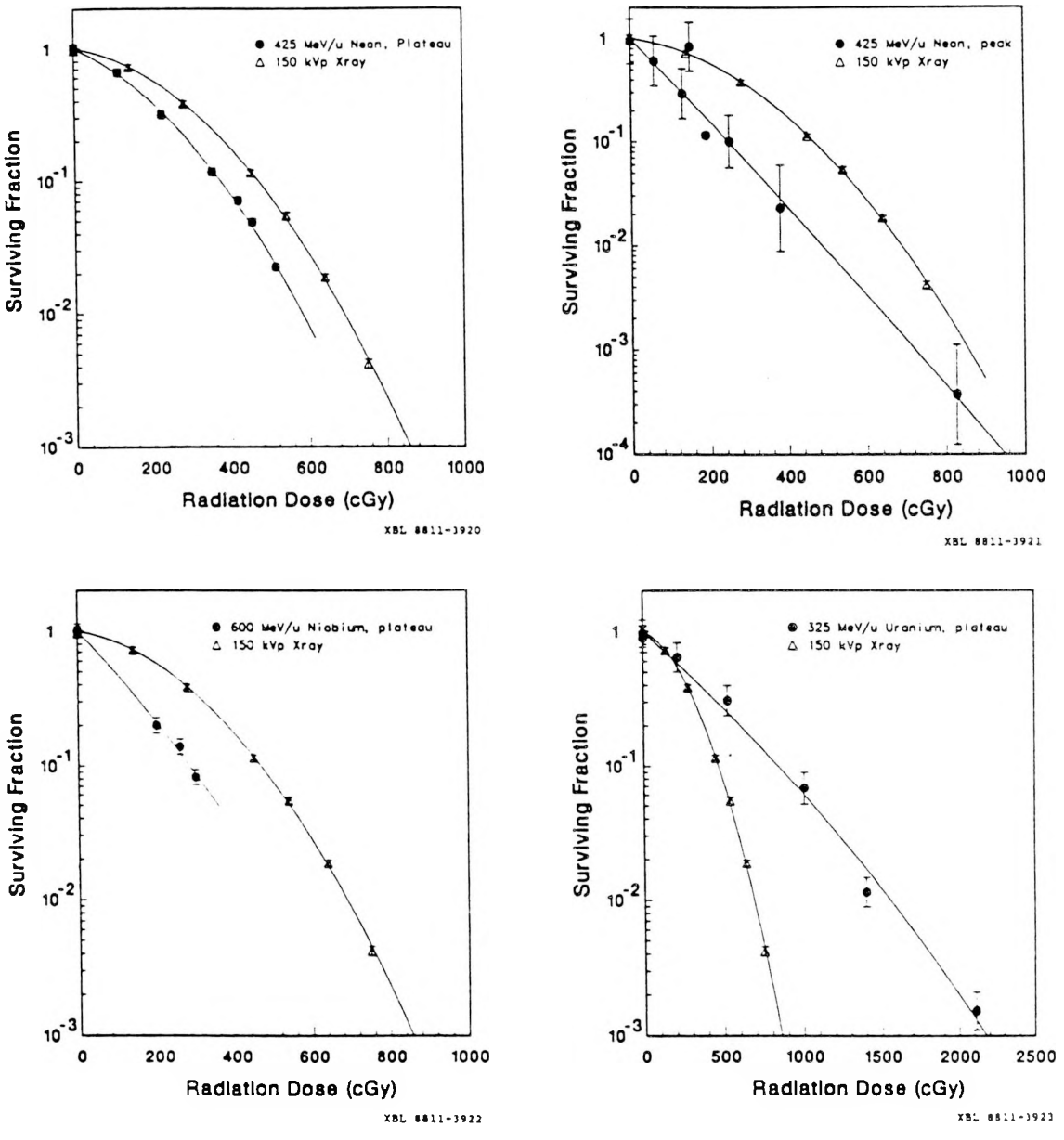


Figure 3. CHO-tsH1 survival curves. Cells were grown as confluent, serum-deprived monoloayers in plastic dishes and then exposed to x-rays or one of four heavy-ion particle beams. To facilitate comparisons the x-ray survival curve has been repeated in each panel.

TABLE 2

SURVIVAL PARAMETERS

Linear Quadratic Model

| Beam | Alpha ($x10^{-3}$ $rad^{-1}$) | Beta ($x10^{-6}$ $rad^{-2}$) | P.E. |
|---|---|---|---|
| 150 kVp X-ray | 1.11 ± 0.70 | 8.10 ± 1.10 | .995 ± .081 |
| 425 MeV/u Ne (plateau) | 3.00 ± 1.30 | 8.47 ± 2.60 | .999 ± .120 |
| 425 MeV/u Ne (peak) | 9.15 ± 4.60 | .576 ± 6.20 | 1.06 ± .540 |
| 600 MeV/u Nb | 7.04 ± 30.1 | 3.70 ± 110 | .997 ± 1.60 |
| 325 MeV/u U | 2.45 ± 1.30 | .328 ± .680 | 1.08 ± 0.470 |

Single-hit Multitarget Model

| Beam | N | $D_o$($x10^{+2}$ rad) | P.E. |
|---|---|---|---|
| 150 kVp X-ray | 7.58 ± 8.50 | 1.07 ± .22 | .950 ± .260 |
| 425 MeV/u Ne (plateau) | 2.95 ± 2.20 | 1.09 ± .18 | .984 ± .210 |
| 425 MeV/u Ne (peak) | 1.27 ± 1.40 | 1.00 ± .28 | 1.01 ± .570 |
| 600 MeV/u Nb | 1.26 ± 11.0 | 1.13 ± 3.80 | .999 ± 1.70 |
| 325 MeV/u U | 2.09 ± 1.80 | 2.90 ± .440 | .993 ± .320 |

Parameters calculated from best fits to survival data (Albright, 1988). Alpha is the coefficient of the linear term and beta the coefficient of the quadratic term in the linear-quadratic model. N is the number of targets in the single-hit multitarget model and $D_o$ is the reciprocal of the slope of the exponential portion of the survival curve. P.E. is the average plating efficiency, a parameter introduced to provide a better fit to data by not forcing the surviving fraction to pass through 1 at zero dose. The error associated with each parameter refers to a 95% confidence interval.

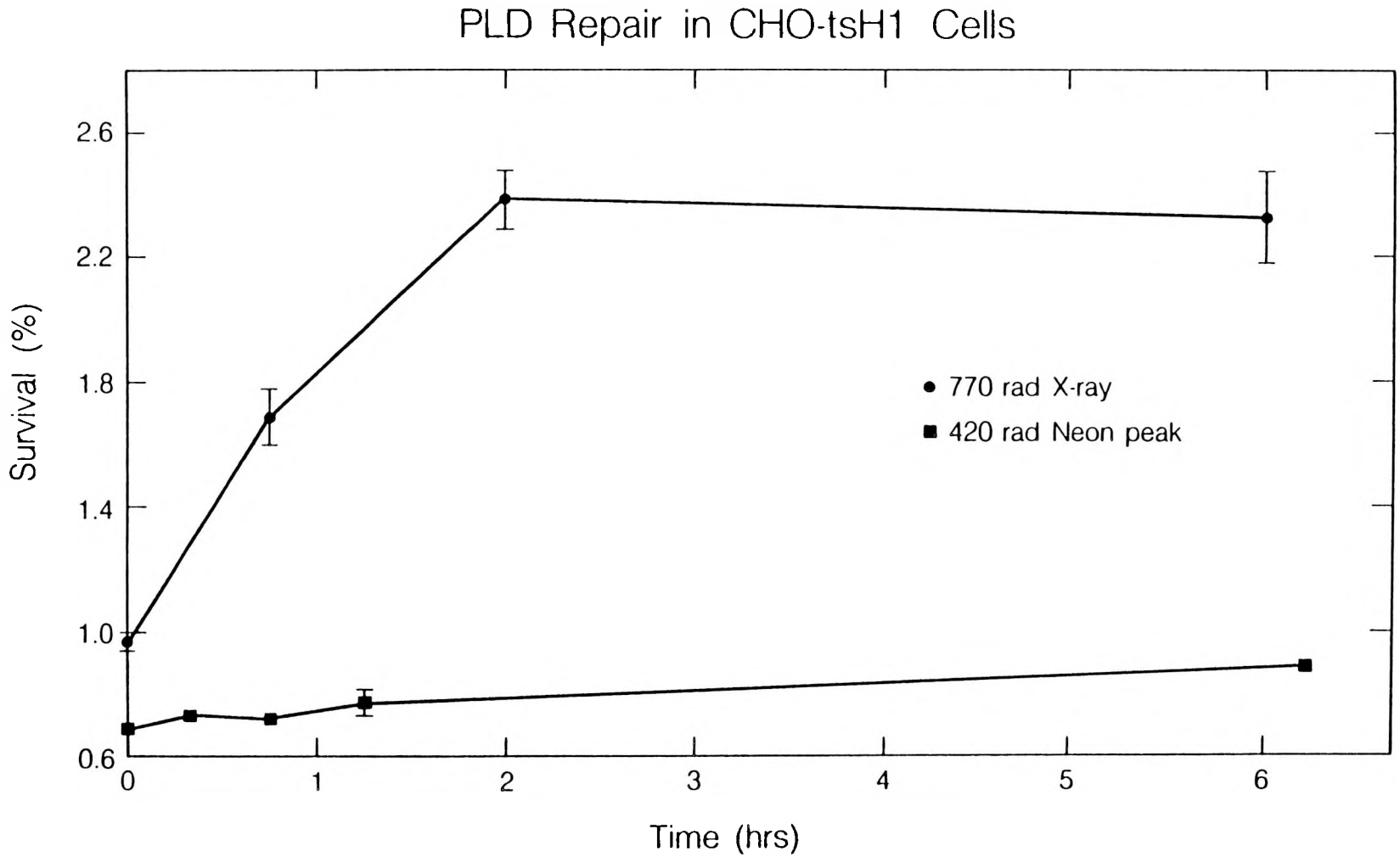


Figure 4. PLD repair in CHO-tsH1 cells. The figure shows the extent of recovery in cells exposed to either 770 rad x-rays or 500 rad Ne-peak ions during post-irradiation incubation at 35°C.

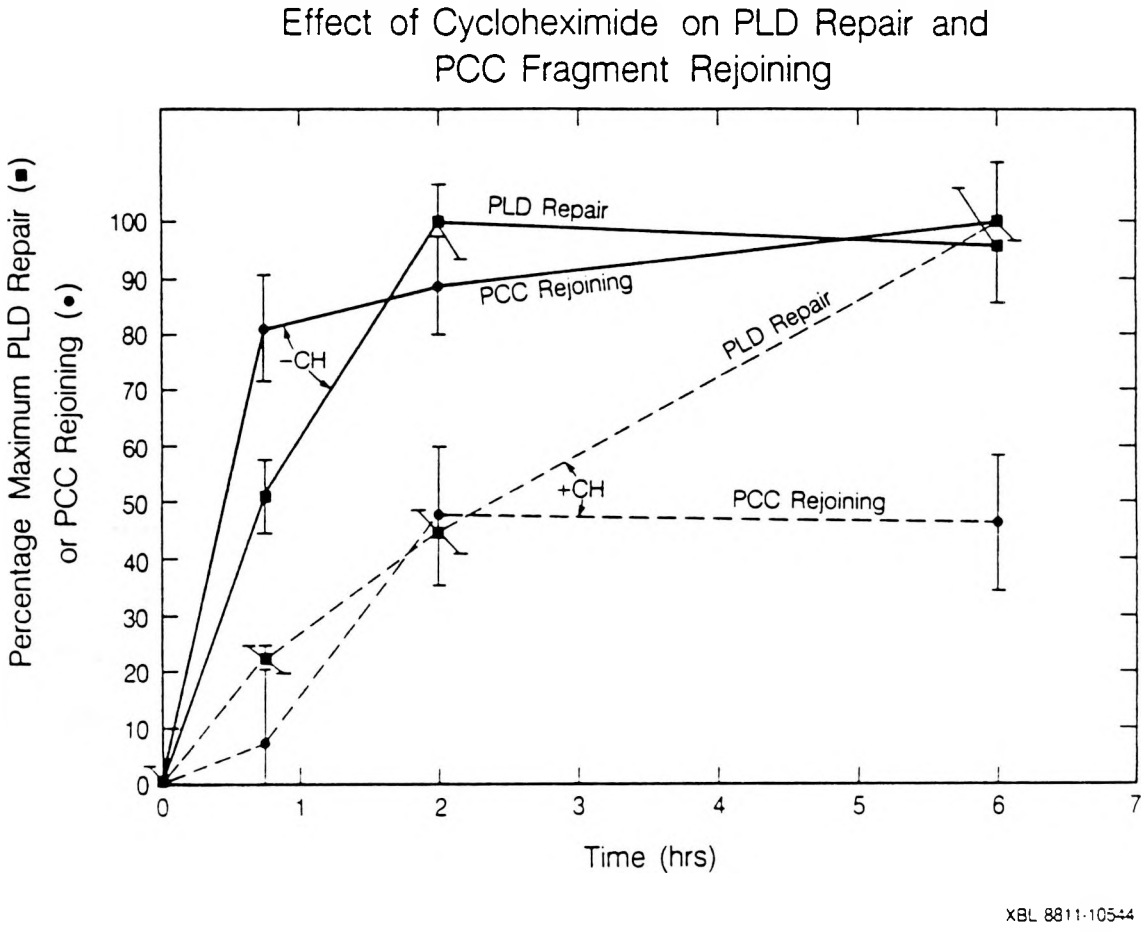


Figure 5. The effect of cycloheximide on PLD repair and PCC fragment rejoining. The data are expressed as a percentage of either the maximum increase in survival or maximum extent of PCC fragment rejoining that occured during the repair period.

25 µg/ml cycloheximide for 6 hours at 35°C while the other was processed immediately. The 0 hr sample had an average of 21.0 PCC fragments per cell (0 breaks) while the 6 hr. sample had 21.5 PCC fragments per cell (0.5 breaks). A "t" test indicated that there was no significant difference at the $p = .05$ level between the two samples. Thus cycloheximide apparently does not produce significant chromatin breakage even after a 6 hour exposure, which is much longer than the time required to complete the PCC process in the course of an ordinary experiment. In addition to cycloheximide treatment, samples were placed on ice both before and after irradiation to further inhibit cellular repair processes that might have reduced the number of chromatin breaks before the procedure was completed. These experimental conditions provided a significant improvement over early trials of the PCC technique where ice and cycloheximide were not used. To ensure that some aspect of the PCC technique was not inducing breakage in unirradiated cells, zero-dose controls were performed for most of the experiments reported here. Mitotic CHO-tsH1 cells have a distribution of chromosomes that is symmetrical about 21 per cell. Several of the PCC controls had a mean number of PCC fragments slightly greater than 21, but in no case was the mean larger than 21.2. To test for a significant difference between the means of the distribution of mitotic chromosomes and the zero-dose distribution of PCC fragments the "t" test was applied. In no single experimental control, nor in the pooled results of all controls, could a significant difference be found at the $p = .05$ level.

Figure 6 shows the initial yield of chromatin breaks per cell per unit energy absorption as a function of LET. The curve has a nearly flat plateau at low LET values followed by a rise to a broad peak in the 100-200 keV/µm range and then a continuous decline thereafter, eventually falling well below the plateau level. At the high LET end of the curve,

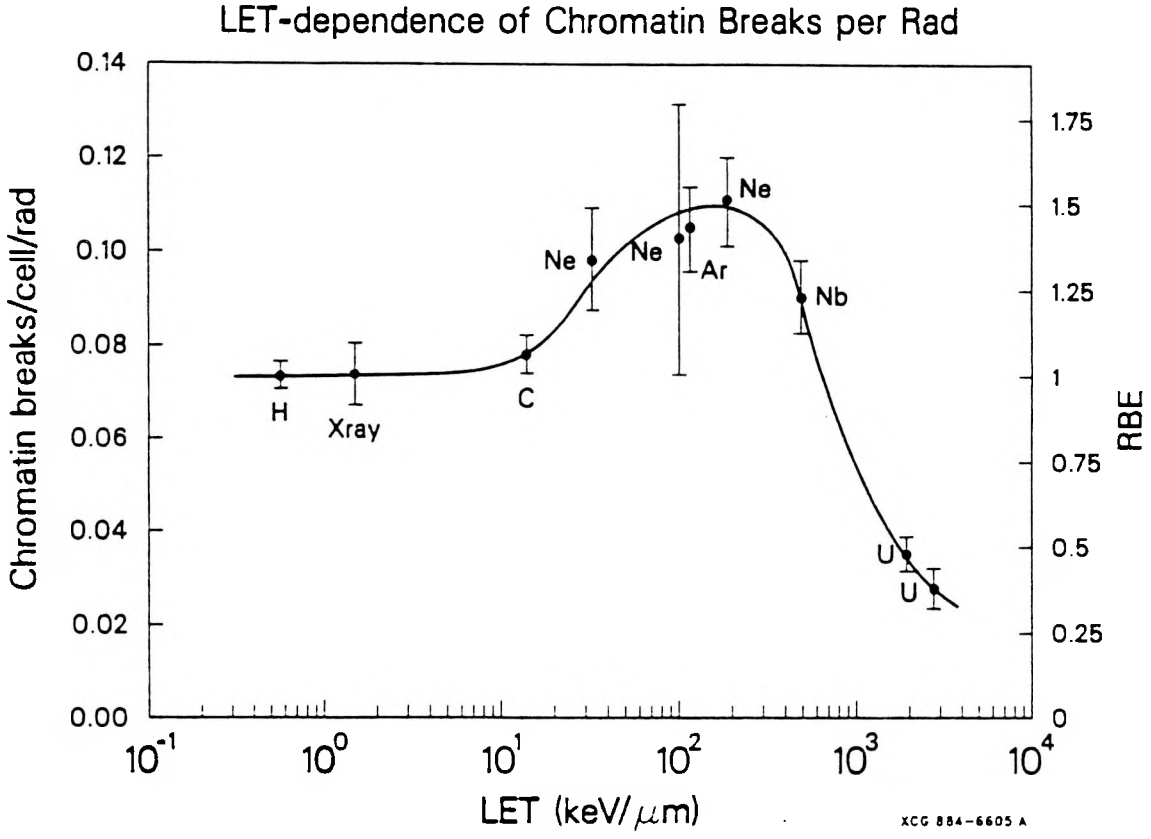


Figure 6. The yield of chromatin breakage. The vertical axis on the left-hand side of the figure refers to the yield per unit energy absorption while the right-hand side shows the RBE with the x-ray yield as reference.

the two uranium beams are most notable for their inefficiency at breaking chromatin. The same data set can be considered from another perspective, the average breakage yield from single particle traversals of the cell nucleus. To make this conversion of the data set one needs to know the fluence of particles which passed through the nucleus. The major and minor axes of 20 elliptically-shaped CHO-tsH1 cell nuclei were measured. The cross-sectional area, as calculated using the equation for the area of an ellipse, was found to be 112.5 ± 12.2 $\mu m^2$ (mean ± standard deviation). Given the LET of a particle beam in keV/μm the number of particles passing through a 1 $cm^2$ area per rad of exposure is 6.242 x $10^6$/LET (Bevalac Users' Handbook). Therefore, the fluence of particles which passed through a CHO-tsH1 cell nucleus from a dose of D rads is 7.022 D/LET. Figure 7 presents the same data as Figure 6 but displayed as the average yield of chromatin breakage from single particle traversals as a function of LET. On this log-log plot the slope is 1 at the lowest LET values. The slope rises slightly with each incremental increase in LET above the proton point. There is an inflection point, whose exact position is difficult to determine on the gently curving line, somewhere between 40 and 90 keV/μm. Above the inflection point the slope decreases with increasing LET. The maximum slope of this sigmoidal curve is ~ 1.3 at the inflection point. The slope decreases to 1 at a point within the 100 to 200 keV/μm range. The curve appears to be reaching a plateau at the very highest LET values, but this is not demonstrated conclusively by the data. In CHO-tsH1 cells grown as a confluent monolayer, there is an average of 1 chromatin break from a single particle traversal of the cell nucleus at an LET of ~ 65 keV/μm. This value is at or near the inflection point. The PCC data from which Figures 6 and 7 were constructed can be found in Table 3. Figure 8 shows the dependence of chromatin breakage on particle fluence for the Ar,

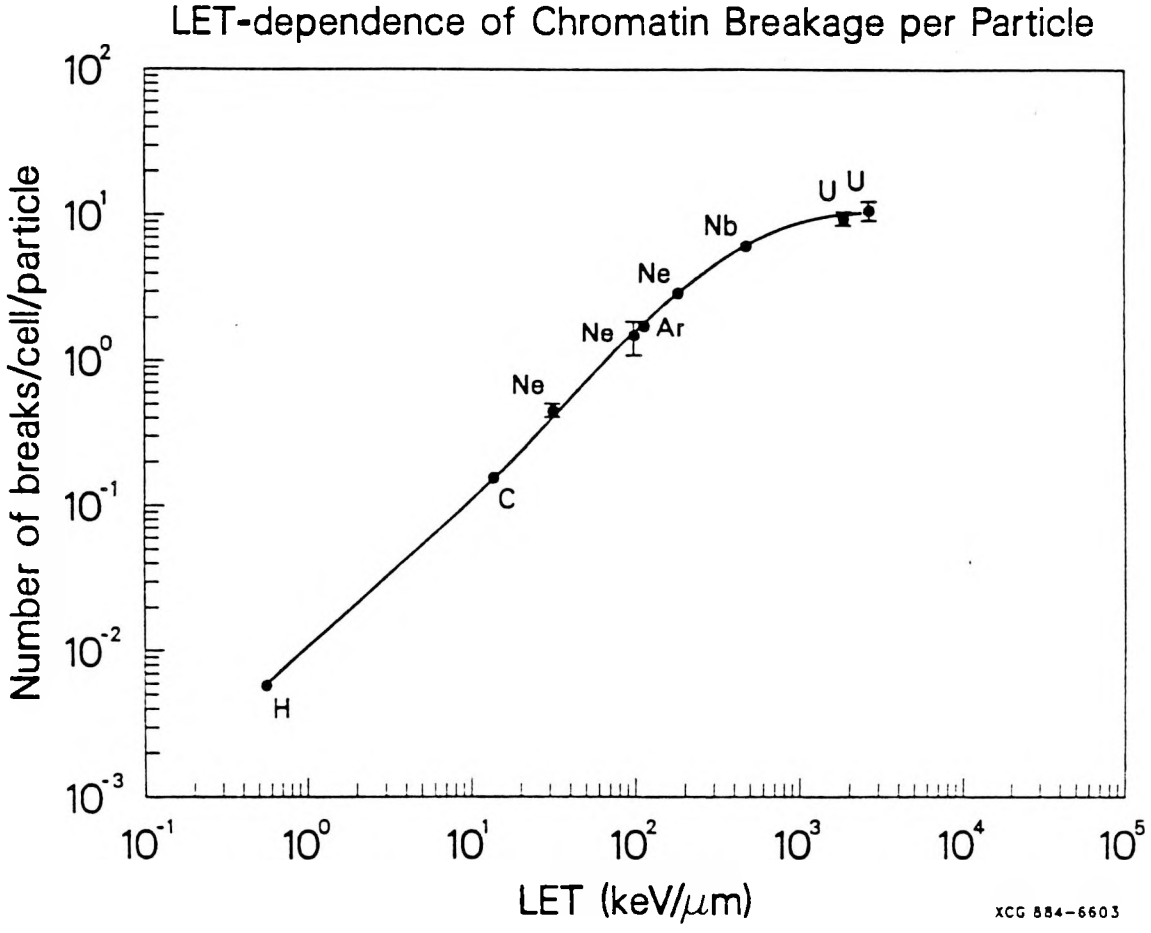


Figure 7. The average yield of chromatin breakage from single particle traversals of the cell nucleus.

TABLE 3

INITIAL YIELD OF CHROMATIN BREAKS IN CHO-tsH1 CELLS

| Beam | LET (keV/μm) | Chromatin Breaks/Cell/Rad | Chromatin Breaks/Cell/Particle |
|---|---|---|---|
| 150 MeV/u H | .562 | .0735 ± .0031 | .00588 ± .00025 |
| 150 kVp X-ray | ~1.5 | .0738 ± .0066 | - |
| 300 MeV/u C | 13.74 | .0780 ± .0042 | .1527 ± .0082 |
| 425 MeV/u Ne (plateau) | 32 | .0983 ± .0107 | .4481 ± .0489 |
| 425 MeV/u Ne-D (near peak) | 100 | .1025 ± .0290 | 1.460 ± .4120 |
| 400 MeV/u Ar | 115 | .1048 ± .0091 | 1.716 ± .149 |
| 425 MeV/u Ne-F (peak) | 183 | .1107 ± .0093 | 2.884 ± .243 |
| 600 MeV/u Nb | 475 | .0902 ± .0058 | 6.101 ± .394 |
| 960 MeV/u U | 1900 | .0351 ± .0036 | 9.508 ± .982 |
| 325 MeV/u U | 2700 | .0279 ± .0043 | 10.72 ± 1.64 |

The average initial level of chromosome breakage in $G_1$ cells as measured by the PCC technique is presented on both a per unit energy absorption basis and a per particle traversal of the cell nucleus basis. The error associated with each value refers to the standard error of the mean.

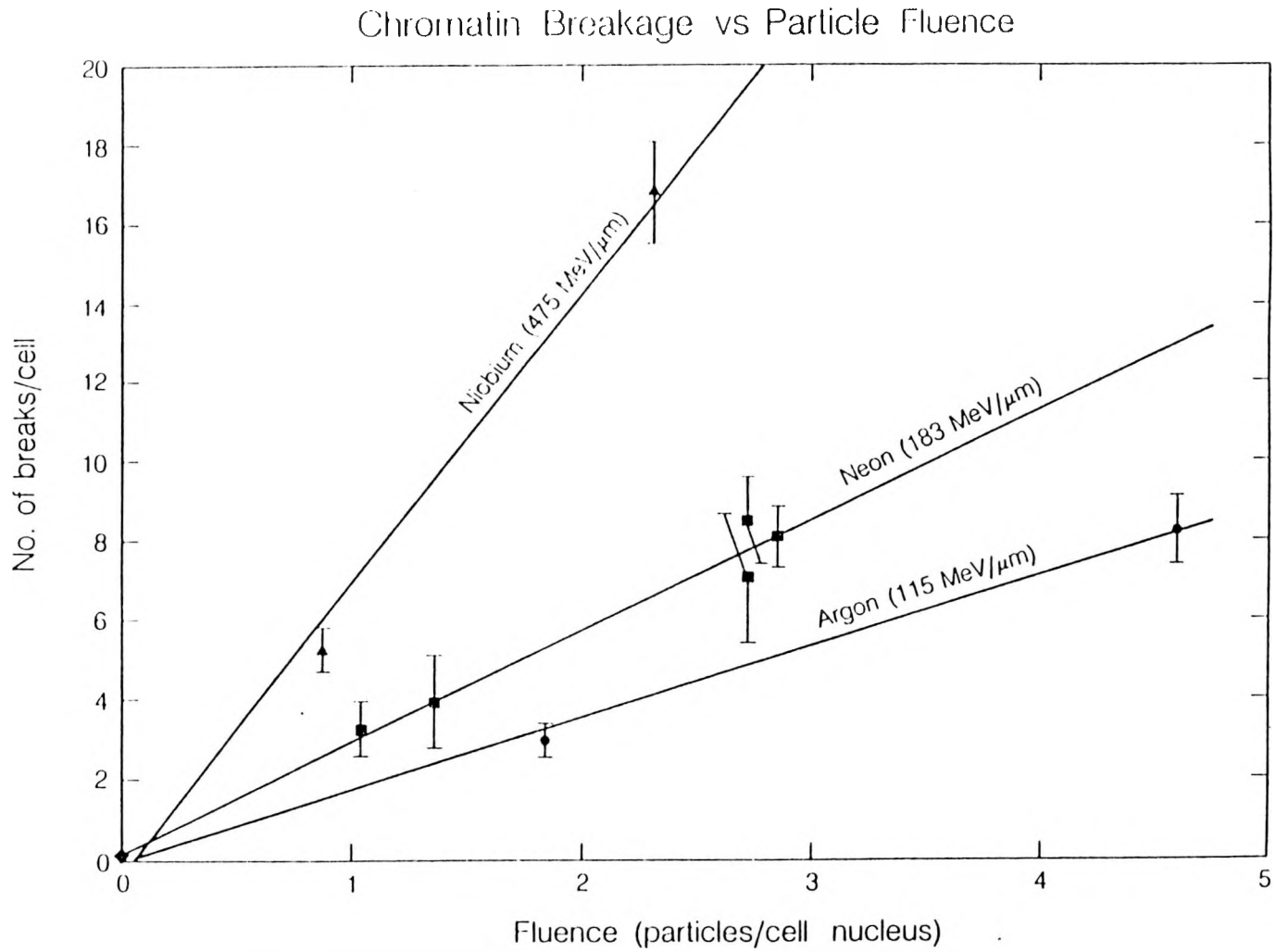


Figure 8. The dependence of the average chromatin breakage yield on particle fluence for three high-LET heavy-ion beams. Straight lines were fitted to the data points by the least-squares method.

Ne-peak and Nb beams. In each case a straight line fit the data points well indicating a linear yield with increasing fluence or dose.

C. Chromatin Breakage, Initial Distribution

Since the PCC technique can detect chromatin breaks in individual cells, it is possible to analyze the distribution of this kind of lesion. DNA strand break assays which homogenize the entire cell sample cannot do this. Following irradiation with x-rays and low LET particle beams, the initial distribution of chromatin breaks in CHO-tsH1 cells was Poissonian (Table 4). This finding was expected based on the random nature of energy deposition by low LET radiation. As the LET of a particle beam increases, energy deposition can no longer be considered random, rather, there is a much higher energy density close to the trajectories of individual particle tracks (Chatterjee and Schaefer, 1976). In this case it was thought that the distribution of chromatin breaks might deviate from Poisson statistics. The variance-to-mean ratio, the relative variance, is useful as an indicator of the dispersion of a distribution. If chromatin breaks are Poisson-distributed the relative variance is expected to equal 1. By this measure a number greater than 1 may indicate overdispersion. Fisher's dispersion test (Fisher, 1946; Croxton, 1953) was used to determine whether the relative variance is statistically different from 1 at the $p = .05$ significance level. The results of this test for each of the 10 beams used in the thesis work are shown in Table 4. With increasing LET, there is a general trend towards larger values of the relative variance. This trend reflects a monotonic rise in the average number of chromatin breaks per cell produced by single particle traversals of the cell nucleus. When Fisher's test is used with $p = .05$, significant overdispersion occurred for all beams producing in excess of 1 chromatin break/cell/particle. This observation

TABLE 4

DISPERSION OF CHROMATIN BREAKS IN IRRADIATED CHO-tsH1 CELLS

| Beam | LET (keV/μm) | Breaks/Cell/Particle | Relative Variance | Significantly Overdispersed? |
|---|---|---|---|---|
| H | .562 | .00588 | 1.16 | No |
| X-ray | ~1.5 | - | 1.42 | No |
| C | 13.7 | .153 | 1.11 | No |
| Ne | 32 | .448 | 1.41 | No |
| Ne-D | 100 | 1.46 | 3.59 | Yes |
| Ar | 115 | 1.79 | 3.90 | Yes |
| Ne-F | 183 | 2.88 | 5.66 | Yes |
| Nb | 475 | 6.10 | 7.31 | Yes |
| U | 1900 | 9.51 | 10.7 | Yes |
| U | 2700 | 10.7 | 8.47 | Yes |

For each beam used in the thesis work the table shows the LET at the sample position and the average number of chromatin breaks/cell/particle traversal. Also shown is the relative variance, an indicator of the dispersion of chromatin breaks within the irradiated cell population. Fisher's dispersion test was used to determine significant overdispersion (see text). The test revealed that a significant departure from a Poisson distribution occurred whenever the irradiating beam had a tendency to produce multiple chromatin breaks from single particle traversals of the cell nucleus.

depends in part on the stringency of the criterion chosen to indicate overdispersion. The advantage of the $p = .05$ significance level is that it clearly demonstrates an association between the rising yield of chromatin breakage from single particle traversals of individual cell nuclei and the broadening distribution of chromatin breaks in the irradiated cell population. In the calculations presented here, no attempt was made to factor out small components in the overall dispersion due to a naturally occurring spread in chromosome number about the modal value and to the slight additional broadening caused by scoring difficulties. Figure 9 shows the actual distribution of chromatin breaks/cell in unirradiated cells, after low-LET X-irradiation, and after very high-LET uranium-ion irradiation.

D. Rejoining Kinetics of Chromatin Breaks

It was thought that it would be of great interest to determine the cellular response to breaks in chromatin produced by radiations of varying LET. Experiments were designed to measure the level of chromatin breaks after holding irradiated samples at 35° C for various periods of time. All samples were placed on ice both before and immediately after irradiation, but only the 0 hour incubation samples were treated with cycloheximide. Cells were kept on ice during transportation from the Bevalac to cell culture facilites in another building about a half mile away. Just prior to the beginning of the incubation period, cold medium was aspirated from the dishes and warm conditioned medium was added. Conditioned medium is that medium in which the confluent, serum-deprived cells were growing. The same dose was given to all test samples within an experiment. The initial number of chromatin breaks varied by less than a factor of 2 between the 4 experiments reported here.

# Histograms of PCC Data

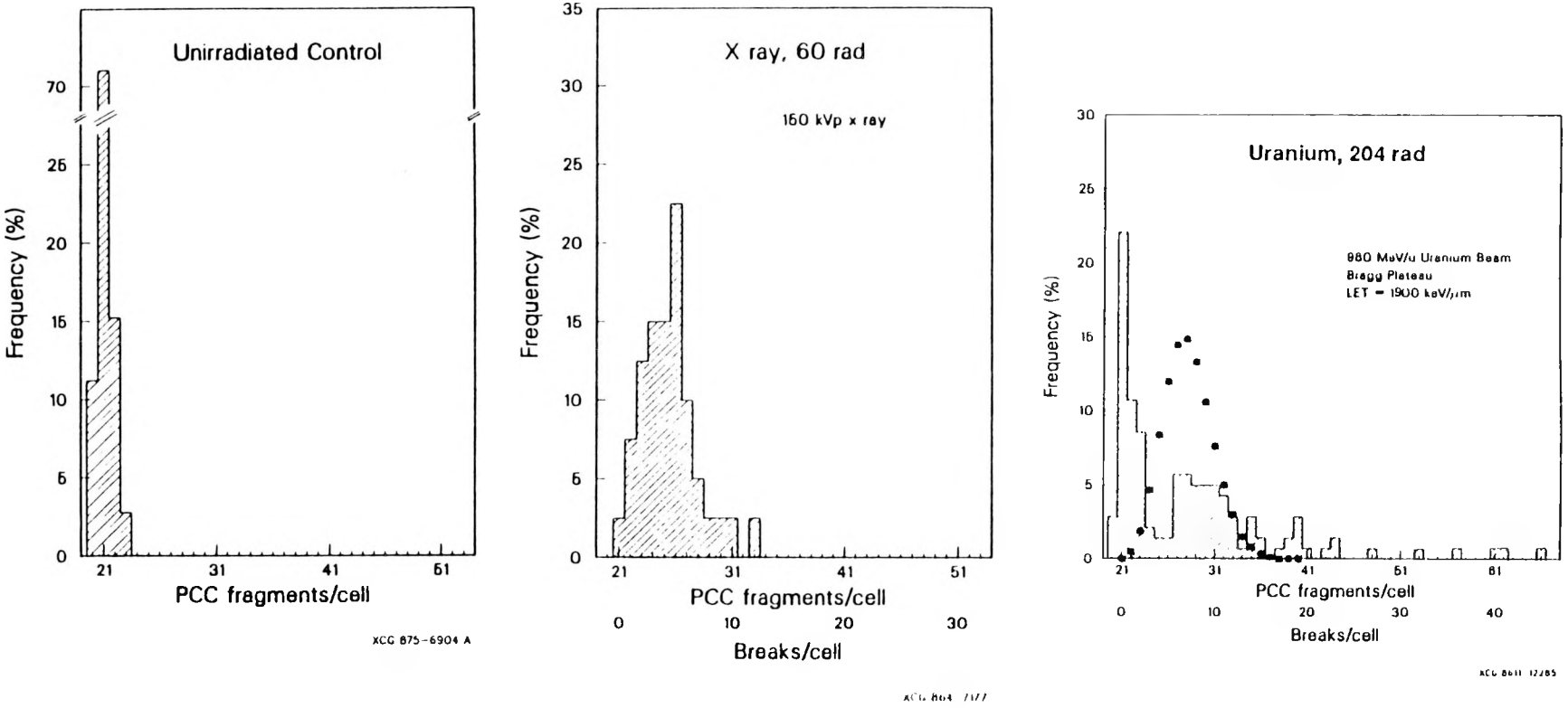


Figure 9. The distribution of chromatin breaks in CHO-tsH1 cells. The horizontal axis gives both the number of PCC fragments/cell and also the number of chromatin breaks/cell which is taken to be the number of PCC fragments in excess of 21, the modal chromosome number. The dark circles in the third panel display the values of a theoretical Poisson distribution having the same mean as the uranium data.

The results, shown in Figure 10, revealed a time-dependent decrease in the average number of chromatin breaks per cell in each experiment. Each data set could be fitted adequately by the equation

$$B(t) = B_r e^{-t/\tau} + B_u \quad (1)$$

where B(t) is the number of chromatin breaks remaining at time t, $\tau$ is the time constant for the first order rejoining process, $B_r$ is the fraction of breaks which rejoin and $B_u$ the fraction that does not rejoin during the interval studied (Table 5). The fast component, $B_r$, shows no clear LET dependence. In addition there is a slow- or perhaps non-rejoining component, $B_u$. This component strongly depends on LET.

Experiments with UV24C2-3 Cells

A. Survival

Confluent, serum-deprived UV24C2-3 cell cultures were exposed to graded doses of either x-rays or accelerated Ne ions. When plated immediately, the survival curves shown in Figure 11 were obtained. The Ne dose-response curve was exponential. The RBE calculated from these curves at the 10% survival level was 2.1 ± 0.2 ($RBE_{10}$ ± standard error). PLD repair was measured by exposing cell cultures to single doses of either 800 rad x-rays or 500 rad Ne ions and then plating for survival after various incubation periods at 37°C. The results are shown in Figure 12. X-irradiated cells demonstrated a 1.8 x increase in survival during the repair period. No recovery was observed after the Ne dose within the 6 hr. interval studied.

B. Chromatin Breakage, Initial Yield

The PCC technique was used to determine the efficiency with which x-rays and Ne ions induce breakage in cellular chromatin. Cultures were irradiated on ice with either 240 rad of x-rays or 165 rad of Ne ions and then processed immediately. It was found that x-rays induce breakage at

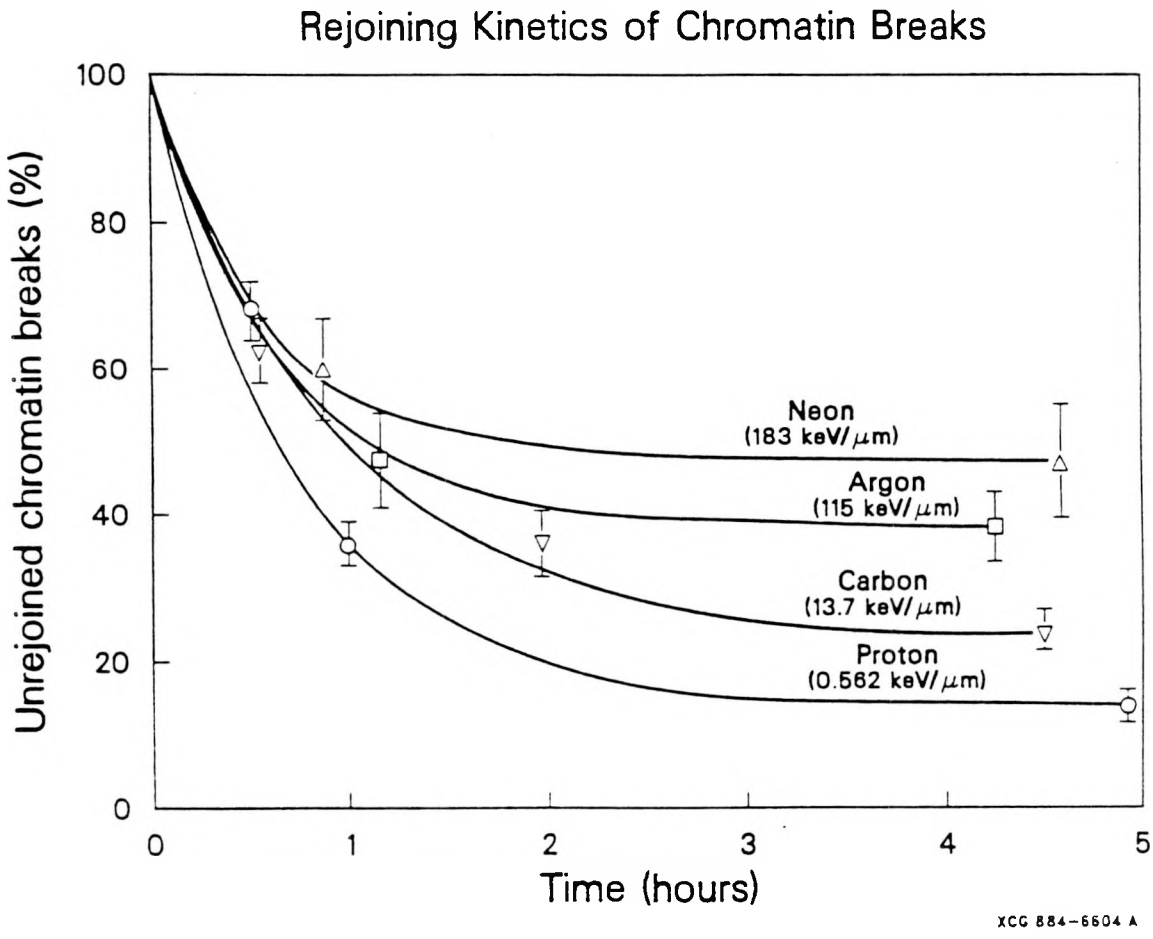


Figure 10. The time course of the chromatin-break rejoining process in CHO-tsH1 cells. The figure shows the percentage of breaks remaining after a specified post-irradiation incubation interval. Using equation (1) curves were fitted to the data points with values for the parameters taken from table 5.

TABLE 5

KINETICS

| Beam | LET(keV/μm) | τ(min) | $T_{1/2}$(min) | $B_r$ | $B_u$ |
|---|---|---|---|---|---|
| H | .562 | 44.3 | 30.7 | .863 | .137 |
| C | 13.7 | 56.0 | 38.8 | .769 | .231 |
| Ar | 115 | 39.9 | 27.6 | .620 | .380 |
| Ne(peak) | 183 | 39.6 | 27.5 | .529 | .471 |

The data were fit to an equation of the form $B(t) = B_r e^{-t/\tau} + B_u$. $B(t)$ is the fraction of unrejoined chromatin breaks at time t, τ is the time constant of the rejoining process and $B_u$ is the residual fraction of chromatin breaks remaining unrejoined after several hours. Also shown is $T_{1/2}$, the time required for half of $B_r$ breaks to rejoin. In an analysis of this kind, the time constant depends strongly on the value chosen for $B_u$.

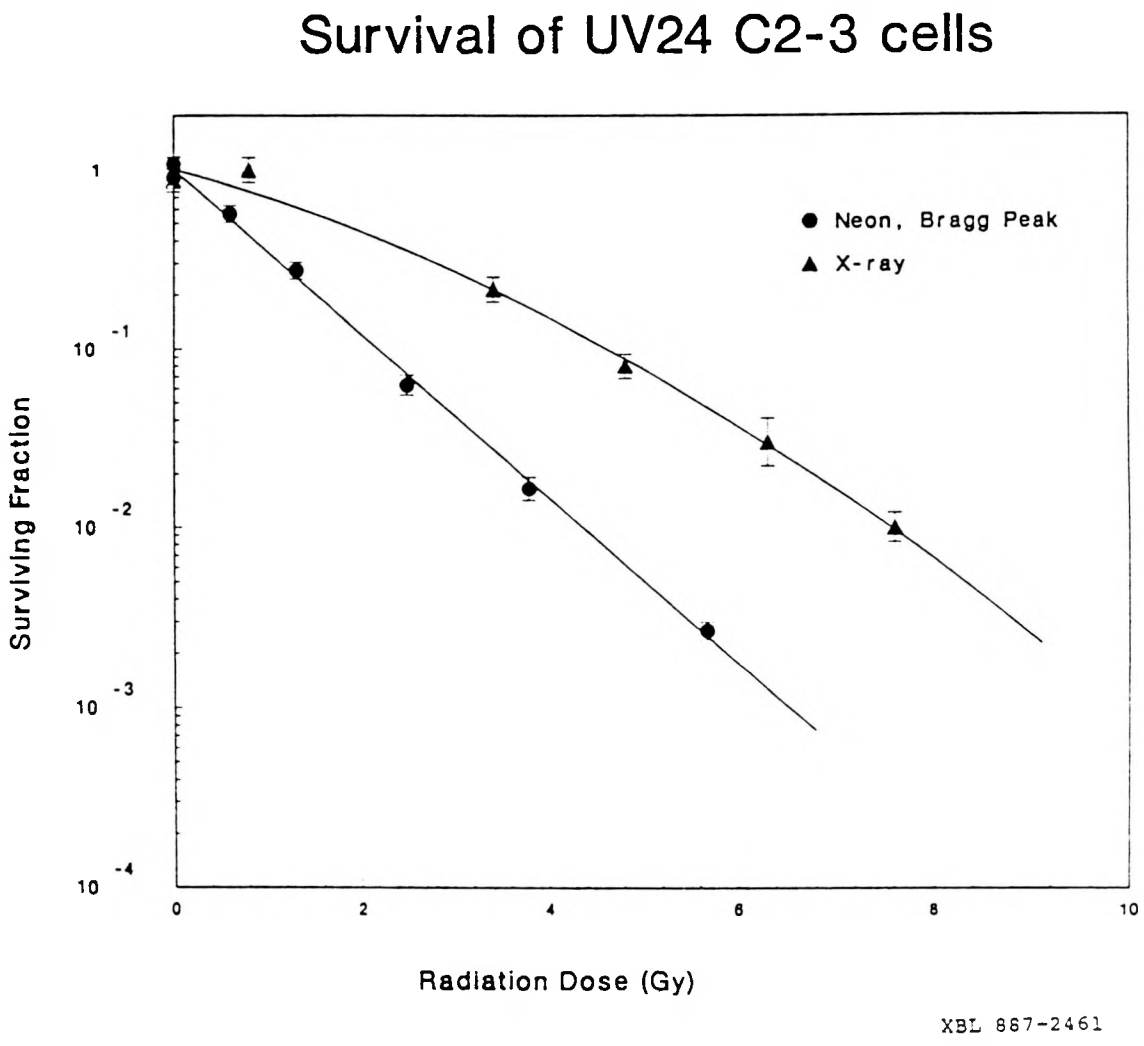


Figure 11. The survival dose response of confluent, serum-deprived UV24C2-3 cells exposed to either x-rays or Ne-peak ions. Linear-quadratic survival curves were fitted to the data points (Albright, 1987).

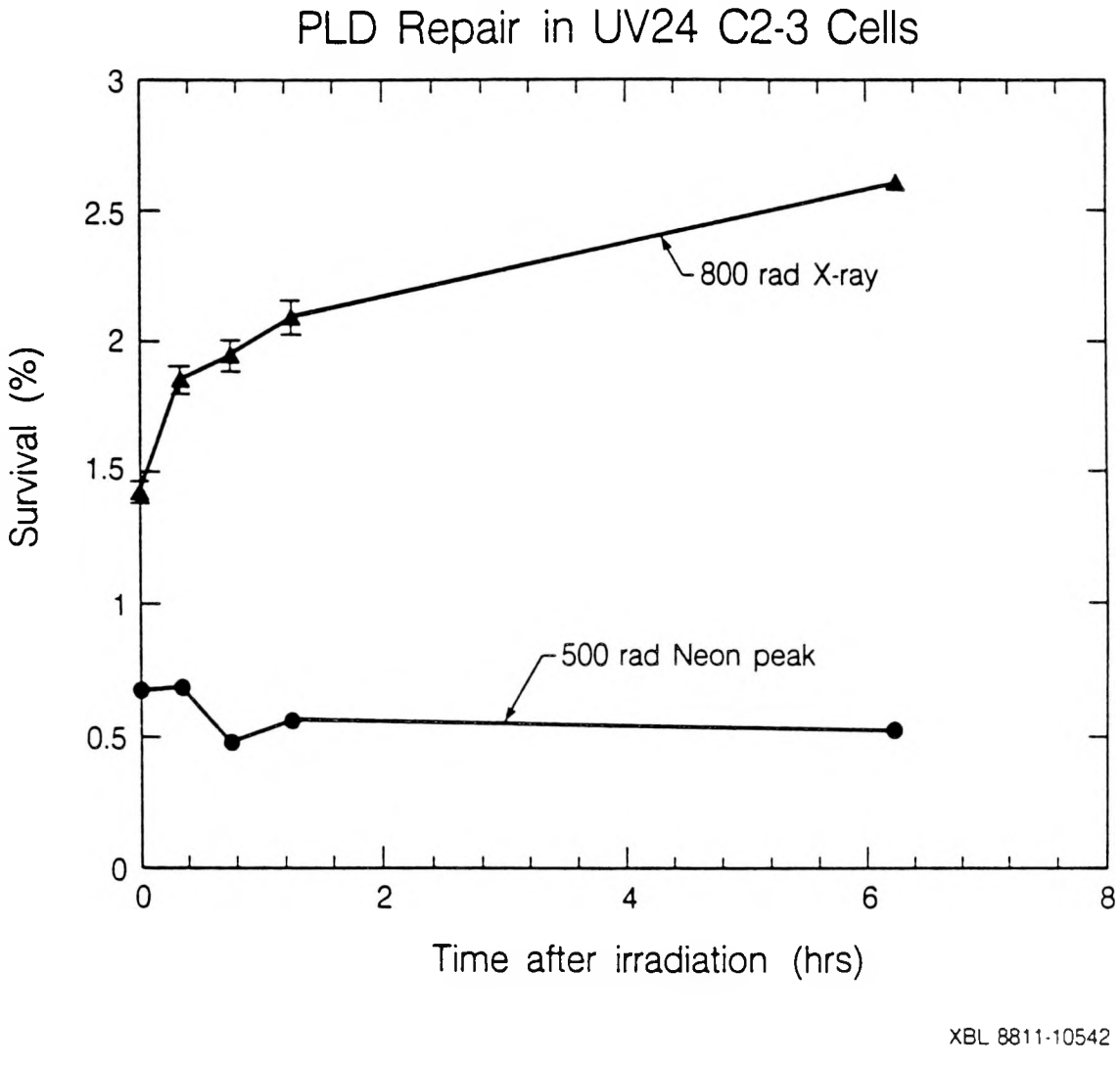


Figure 12. PLD repair in UV24C2-3 cells. Cells were exposed to either 800 rad x-rays or 500 rad of Ne-peak ions and plated for survival after various incubation intervals at 37°C.

the rate of 0.0754 ± .0039 (mean ± standard error) chromatin breaks/cell/rad. Ne ions produce 0.1138 ± .0090 breaks/cell/rad. Compared to x-rays, the Ne beam was 1.5 times more effective.

In one experiment microscope slides were fluorescently stained after in situ hybridization with a human genomic probe. PCC fragments of the human #2 chromosome fluoresce yellow and are easily distinguished from hamster PCC fragments which fluoresce red after counterstaining with propidium iodide. The dose response determined for breakage in the human chromosome (only) after x- or Ne-irradiation is displayed in Figure 13. Straight lines were fit to the data points by the least-squares method. The slope of the x-ray curve was 0.0018 ± .0002 breaks/chromosome/rad and the slope of the Ne curve was 0.0041 ± .0002 breaks/chromosome/rad.

C. Rejoining Kinetics of Chromatin Breaks

The rejoining kinetics of chromatin breaks were determined by allowing various postirradiation repair intervals prior to inducing PCC. The data, shown in Figure 14, are expressed as the percentage of chromatin breaks remaining after a dose of either 1600 rad x-rays or 1062 rad Ne ions. Because of the large number of PCC fragments produced by these high doses, it was necessary to estimate the initial (0 hr) yield based on a linear extrapolation of measurements made at lower doses. Each data set could be fit adequately by the equation $B(t) = B_r e^{-t/\tau} + B_u$. For the x-ray curve; $B_r = 0.891$, $B_u = 0.109$ and $\tau = 23.6$ minutes. For the Ne curve; $B_r = 0.507$, $B_u = 0.493$ and $\tau = 28.7$ minutes.

D. Chromosomal Misrepair

Ring chromosome aberrations are perhaps the most easily detectable chromosomal misrepair product to be found in $G_1$-phase cells after inducing PCC. Ring PCC fragments were scored following post-irradiation

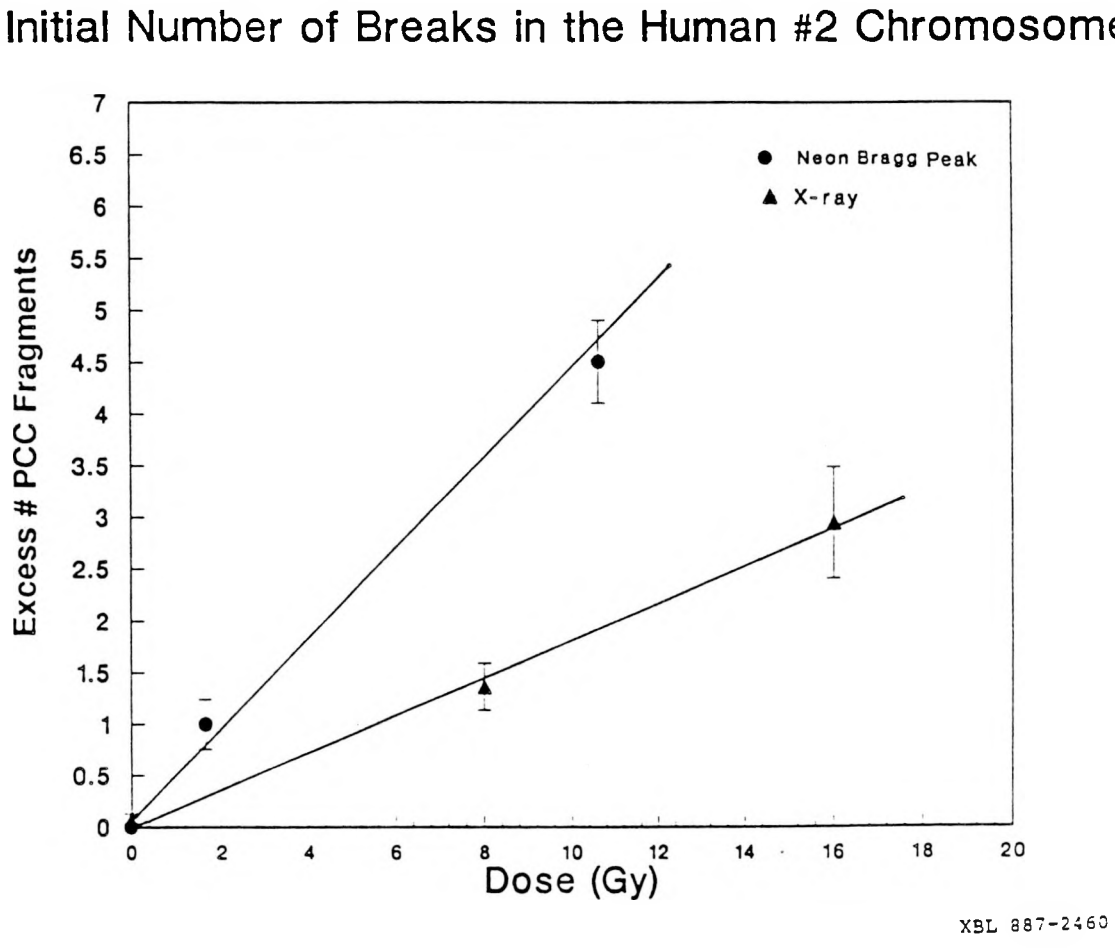


Figure 13. Breakage in the single human #2 chromosome of UV24C2-3 cells. The human chromosome could be differentiated from the hamster chromosomes after fluorescent staining of a hybridized human-genomic DNA probe. Straight lines were fitted to the data points by the least-squares method.

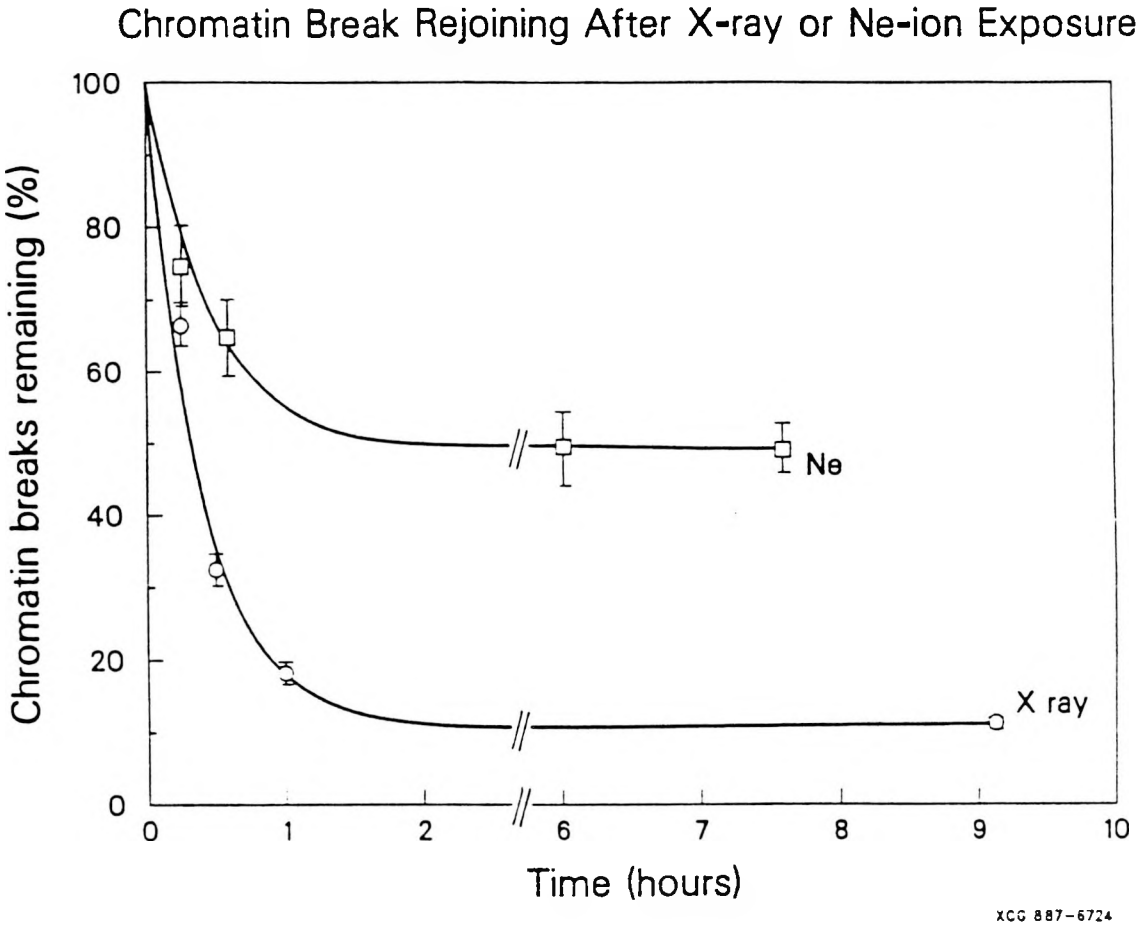


Figure 14. The time course of the chromatin-break rejoining process in UV24C2-3 cells. The percentage of the initial number of breaks remaining is plotted vs repair time. Curves were fitted to the data points using equation (1).

incubation and the data are presented in Figure 15. The doses of 1600 rad x-ray and 1062 rad Ne were chosen to yield a comparable level of initial damage, i.e. ~121 chromatin breaks. Some rings had already formed at the earliest time point observable with the PCC technique. The yield of rings per cell increased steeply during the first hour and more slowly afterwards until an apparent plateau was reached beyond 6 hours. The x-ray data could be fit quite well by an equation of the form

$$R(t) = R_o + R_1 (1 - e^{-t/T}) \quad (2)$$

where R(t) is the yield of rings at time t, $R_o$ the number of rings already present at t = 0, and T the time constant for the first order misrepair process. The best fits found for the constants are: $R_o = 0.15$, $R_1 = 1.15$ and T = 44.5 minutes. The Ne data could also be fitted by the same equation, although not as well, with $R_o = 0.067$ and $R_1 = 0.42$. However, the Ne data are not sufficiently precise to allow a satisfactory estimate of T. Therefore, when drawing the Ne curve, the time constant was arbitrarily set equal to the x-ray value.

The dose response for ring aberrations formed after long incubation times (> 6 hrs) is plotted in Figure 16. Ring aberrations were never seen in unirradiated $G_1$-PCC chromosomes. A quadratic curve of the form

$$R(D) = \alpha D^2 \quad (3)$$

where R(D) is the yield of rings produced by a dose D and $\alpha$ the rate constant, could be fitted to the data. For x-rays, $\alpha = 5.08 \times 10^{-7}$ $rad^{-2}$. For Ne ions, $\alpha = 3.57 \times 10^{-7}$ $rad^{-2}$. The Ne ring data could be fitted equally well by a straight line with slope = $4.05 \times 10^{-4}$ $rad^{-1}$ and intercept = -0.016.

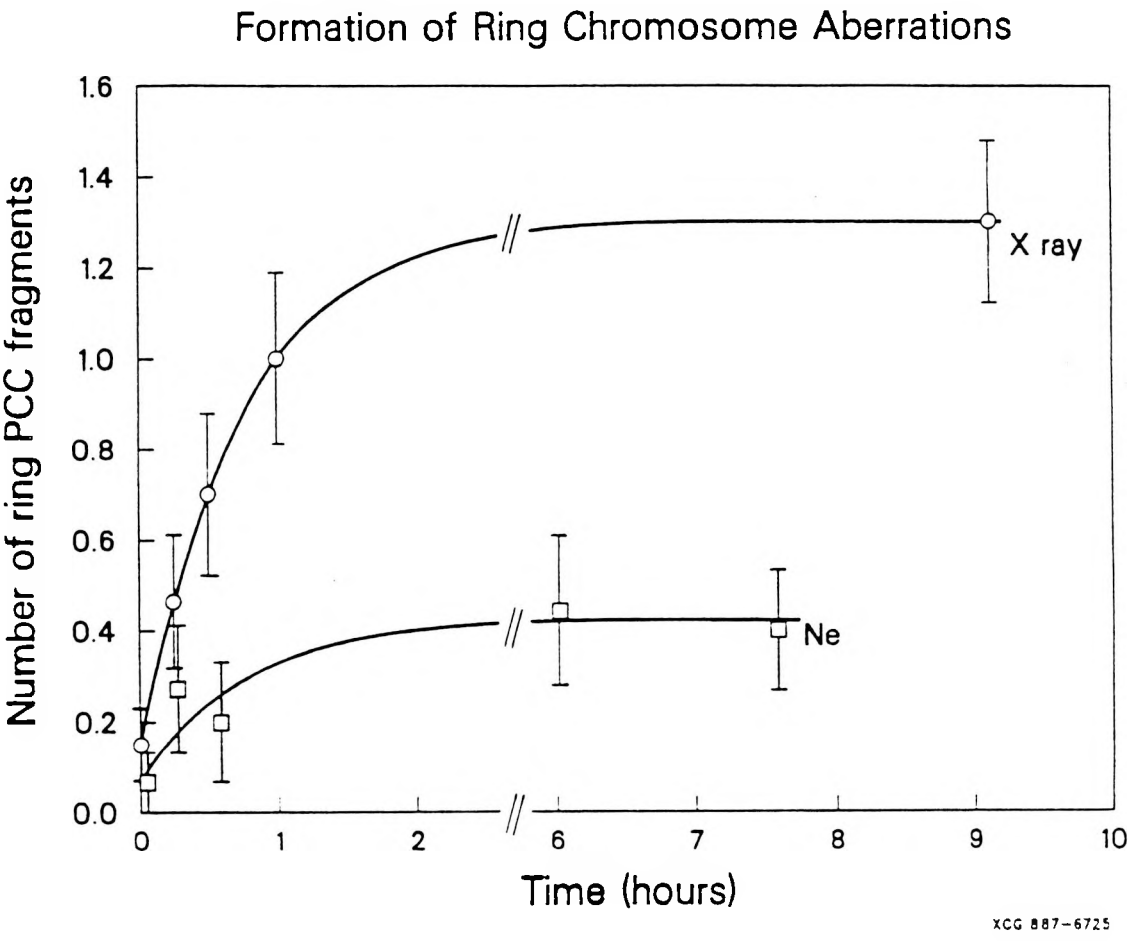


Figure 15. The kinetics of ring chromosome formation in $G_1$-phase UV24C2-3 cells during post-irradiation incubation. Cells were exposed to either 1600 rad x-rays or 1062 rad Ne-peak ions. These doses gave ~121 chromatin breaks initially in either case.

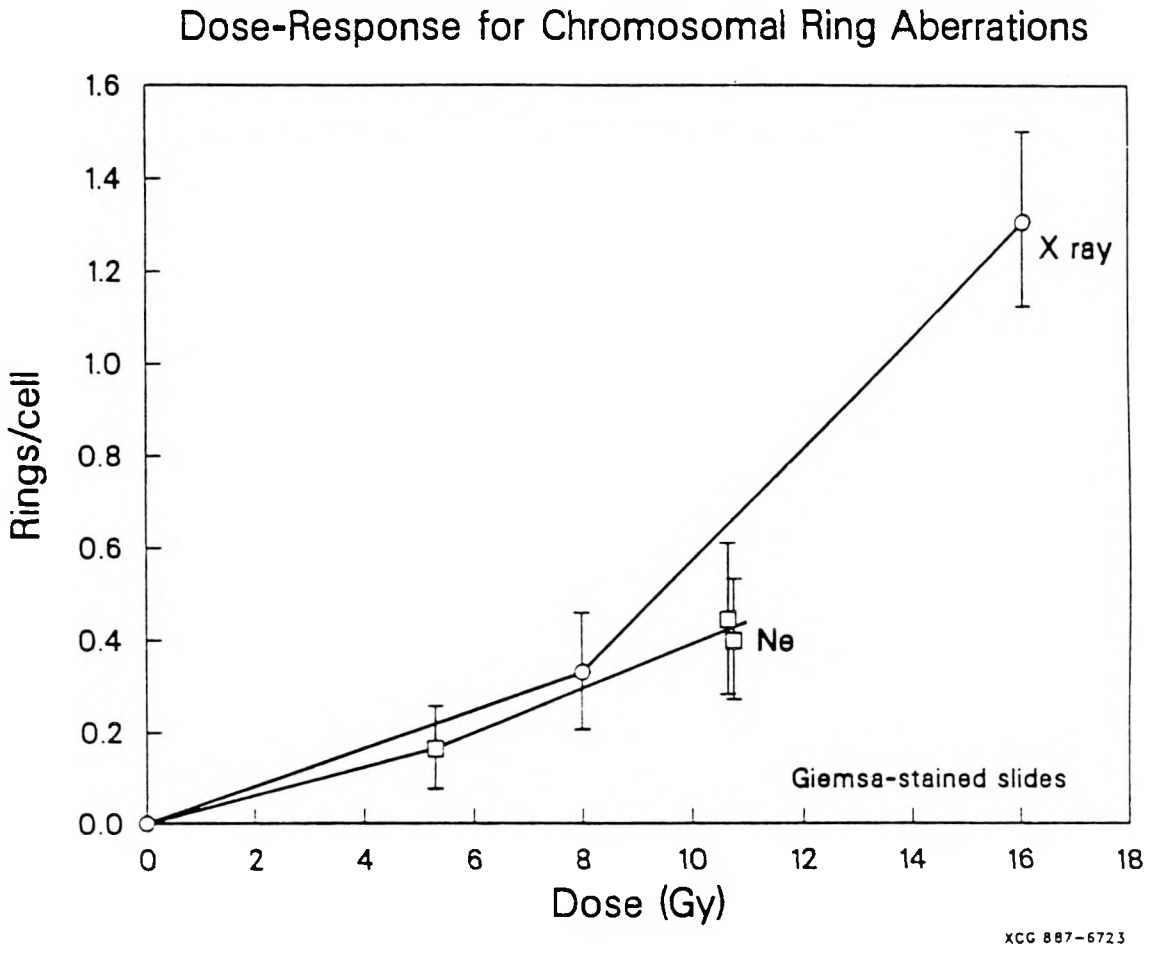


Figure 16. The average number of ring-PCC aberrations scored in UV24C2-3 cells after long post-irradiation repair incubations at 37°C.

# DISCUSSION

Despite many years of investigation of LET-dependent cellular damage very few data exist to assess early effects at the chromosomal level or subsequent modification by repair processes. This deficiency has been addressed by applying the PCC technique to mammalian cells irradiated with x-rays and charged particle beams of various atomic numbers and velocities. The result of this work has been the accumulation of the most extensive data set currently available for the purpose of evaluating $G_1$-interphase chromosomal damage and repair as a function of LET. Original findings obtained from these studies fall into four areas of interest and will be reviewed separately. Finally, some implications of these results for cell survival will be discussed.

## LET Dependence of Initial Chromatin Breakage

The radiation-induced yield of nonrejoining DNA strand breaks measured under alkaline conditions was shown to possess a LET dependence (Ritter et al., 1977; Roots et al., 1979). The initial yield of dsb per unit dose was also found to depend on LET when measured intracellularly (Kampf and Eichhorn, 1983; Aufderheide et al., 1987). In these studies the RBE for strand breakage rose to a peak at ~ 100 keV/μm. Fewer data exist for initial chromatin breakage. Bedford and Goodhead (1987) used the PCC technique to demonstrate a RBE of ~ 2 after α-particle irradiation (130 keV/μm). Xian-Li and Ngo (1988) found a RBE ~ 2.4 for chromatin breakage after fast neutron irradiation. Both of these PCC studies found a linear dose response for the induction of breaks. Several investigations have shown that low LET x-rays induce chromatin breakage linearly with dose (Waldren and Johnson, 1974; Cornforth and Bedford, 1983b; Pantelias and Maillie, 1985).

To determine the dose response for chromatin breakage induced by heavy-ion particle beams, the PCC technique was applied to CHO-tsH1 cells

exposed to Ar, Ne-peak and Nb ions. As with x-rays, heavy ions induced chromatin breaks apparently linearly with dose (Fig. 8). The usefulness of the PCC technique at high doses has been limited by the difficulty of accurately scoring cells containing a large number of very small chromosome fragments. The single human #2 chromosome in the UV24C2-3 cell line accounts for ~ 4% of total cellular DNA. In situ hybridization plus fluorescent staining makes possible the specific detection of human PCC fragments which, because of a much smaller target size, are not too numerous to be accurately scored even at relatively high doses. The linearity of the dose response for initial chromatin breakage was confirmed by this method within, and somewhat beyond, the dose range typically employed in cell survival studies (Fig. 13). Considering the smaller target size, the breakage rate after Ne irradiation was found to be just 10% less than what was predicted based on measurements of breakage in the total genome made at lower doses with Giemsa staining. After x-rays, however, the breakage rate in the human chromosome was almost 40% less than anticipated. While part of the deficit may be due to repair, at least part of the shortfall remains unexplained. It is of some interest to note that if eukaryotic chromosomes were composed of circular DNA molecules (as are the genomes of some lower life forms) then the dose response for chromatin breakage measured by PCC would not be linear at low doses since the first break in each chromosome would not produce an additional PCC fragment.

The work presented in this thesis clearly demonstrates a LET dependence for initial chromatin breakage in CHO-tsH1 cells. The yield per unit dose vs LET curve (Fig. 6) shows a plateau at the lowest LET values, and a rise to a peak in the 100-200 keV/μm range. A maximum RBE of 1.5 was found at the peak. Beyond the peak there is a progressive loss in the effectiveness of particle beams. High energy particles with

a LET of 630 keV/μm would produce no more breaks per unit dose than x-rays. As a consequence of the low breakage efficiency of very heavy high LET particles, atomic fragments produced in nuclear collisions will be more effective per unit dose than the parent nuclei. Even a relatively small amount of fragmentation can lead to a significant overestimation of the breakage potential of a beam like 325 MeV/u uranium ions. The maximum RBE of 1.5 is less than the values of 2 and 2.4 observed by Bedford and Goodhead (1987) and Xian-Li and Ngo (1988) for α-particles and fast neutrons. The differences may be related to track structure effects. For example, even though the LET values are about the same, the energy density in the core of the α-particle tracks was ~ 240 x higher than in the track cores of the Ar ions used in the thesis work. The intracellular dsb data (Kampf and Eichhorn, 1983; Aufderheide et al, 1987) had a maximum RBE of ~5. Here too the high RBE may be due to track structure effects since low energy particle beams were used in the dsb work.

The initial yield of chromatin breaks was measured for UV24C2-3 cells exposed to x-rays or Ne ions at the Bragg peak. These values when compared to the breakage yield in CHO-tsH1 exposed to the same radiations were found to be nearly the same. Comparisons can also be made to low LET chromatin breakage yields obtained by others in $G_1$, cells. The yield of breaks observed in the two cell lines used in the thesis work was slightly greater (~20%) than those found by Cornforth and Bedford (1983a) and Pantelias and Maillie (1985) who used human cells, but 2.8 x greater than the value found by Xian-Li and Ngo (1988) and 3.7 x greater than the value found by Illiakis et al (1988) who used hamster cells. These differences are as yet unexplained but may be due to variations in the amount of repair that takes place during the PCC procedure, cell line characteristics, differences in growth conditions, or differences in

scoring technique. While the various researchers are apparently capable of obtaining consistent results within their own experimental systems, caution is advised when comparing the data obtained by different research groups.

A possible explanation for the observed LET variation in chromatin breakage might be that a DNA dsb alone is not sufficient to break the chromatin fiber. In addition it may be necessary to damage protein in the vicinity of a DNA dsb to have expression of that dsb as a chromatin break. In this hypothesis the increasing chromatin breakage RBE is due solely to the greater localized damage caused by the passage of a high LET ion through a chromatin fiber. However, the similarity between the overall shapes of the DNA dsb and chromatin breakage vs LET curves argues against this explanation. At least for the high energy beams used in the thesis work, it seems more plausible that a constant, LET-independent fraction of DNA dsb are expressed as chromatin breaks. In this case the chromatin breakage RBE would simply reflect variations in the dsb RBE. In assessing the validity of each of these alternative explanations it would be helpful to have both DNA dsb data and chromatin breakage data for the same cell line irradiated with the same particle beams.

Further insights into initial chromatin breakage can be gained by graphing the data as the average yield of chromatin breaks from single particle traversals as was done in Figure 7. At the lowest LET about 170 H ions must cross the cell nucleus for each chromatin break induced. At about 65 keV/μm particles can produce an average of 1 break per cell. Above 65 keV/μm single particles will often produce multiple chromatin breaks on passing through a cell nucleus. The most effective particle tested, 325 MeV/u uranium, also had the highest LET and produced almost 11 breaks per cell. The curve appears to be approaching a plateau. Breakage per particle may be determined by the number of regions where

track structure overlaps chromatin fibers and by the energy deposited in each overlap region (Tobias et al, 1986). In this hypothesis a plateau occurs when the probability of breaking chromatin in each overlap region approaches 1; any additional energy deposited in an overlap region is wasted. This explanation differs from that of Kraft et al (1987) who suggest radical recombination in particle tracks as the mechanism responsible for decreasing biological effectiveness at high LET.

On the log-log plot of Figures 7 and 18 the breakage-per-particle curve has a slope of 1 in the low LET range where radiation is sparsely ionizing. This observation can be understood within the framework of target theory. Assume that energy is distributed randomly and discretely in the particle track/chromatin fiber overlap regions. Also assume that n or more energy deposits per critical volume are required to break the chromatin fiber. A critical volume may have dimensions smaller than an overlap region. For an average of μ energy deposits per critical volume, the probability of breaking chromatin is

$$P = \sum_{i=n}^{\infty} \frac{\mu^i}{i!} e^{-\mu}$$

The quantity μ is proportional to LET. When P is plotted on a log-log plot vs either μ or LET the slope of the curve will be n in the range where μ is small (Fig. 17). Thus a slope of 1 in the low LET range of Figure 7 indicates that a single energy deposit in a critical volume is sufficient to break a chromatin fiber. If a minimum of two energy deposits were necessary then the slope would have been 2. A slope of 1 also rules out any form of multitarget model. The average size of an energy transfer is ~ 40eV (Chatterjee and Magee, 1980) while the energy of a typical chemical bond in an organic molecule like DNA is ~ 3.6eV. A dsb requires the breaking of at least 2 bonds so 40eV is more than 5 x

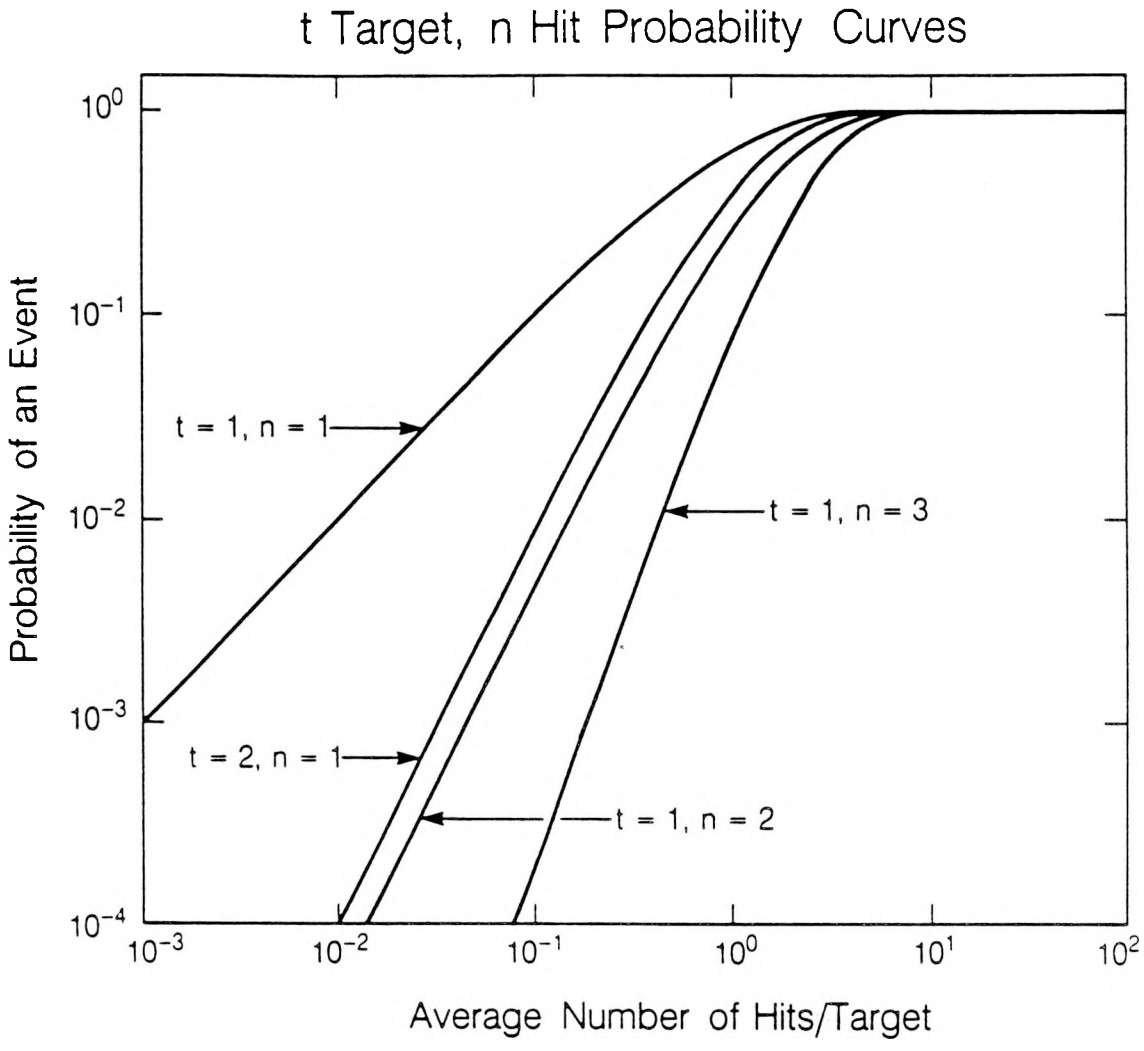


Figure 17. Curves computed from n-hit, t-target models. In each case the limiting slope of the surve is equal to n, the number of hits per target required to produce an event.

the minimum energy needed to sever a DNA double helix. This does not mean that chromatin must necessarily break whenever an energy deposit occurs in a critical volume, only that it will break in some fraction of such occasions. It is likely that there is no effective energy threshold for DNA ds breakage since even the smallest typical energy transfer is large enough to break DNA. Based on an analysis of chromosome aberration data, Neary (1965) and Neary and Savage (1966) also concluded that the initial lesion responsible for aberrations could be produced by a single energy loss event. An RBE >1 in the mid range of the curves in Figures 6 and 7 can also be examined in terms of target theory. For particles of the same velocity, increasing LET implies a larger average number of energy deposits per critical volume. An RBE >1 will occur if the probability of creating a chromatin break from two energy deposits in a single critical volume is greater than the probability of creating a break from two energy deposits each in a separate critical volume. Beyond a certain number, multiple energy deposits per critical volume eventually become wasteful and the RBE decreases. Near the center of low velocity heavy-ion particle tracks the energy density can be extremely high. For these beams it is possible that new "targets", perhaps DNA in heterochromatic regions of interphase chromosomes, may become available for the induction of chromatin breakage. In these targets breakage may require multiple energy transfer events in a critical volume much larger than the diameter of a DNA double helix.

The horizontal axis of Figure 7 could easily be converted from LET to dose since this axis is, in effect, the dose delivered by single particle traversals of the cell nucleus. Doing this leads to an interesting paradox. A linear increase in chromatin breakage was observed when dose was increased by increasing particle fluence but a sigmoidal response was found when dose was increased by increasing the LET of a fixed number of

particles. A resolution to this paradox comes from considering the size of the likely critical target for chromatin breakage - DNA. To break DNA at a specific point energy must be deposited within, or very close to, the double helix at that point. Therefore it is expected that the critical volume would have dimensions on the order of 20Å, the diameter of the DNA double helix. Most of the energy in a particle track is located very close to the center of the track. At biologically relevant doses it is unlikely that two particles will pass through the cell nucleus close enough together to transfer a significant amount of energy to the same small critical volume. A linear dose response results from increasing particle fluence since the effect of each particle is independent of the others. In contrast, increasing the LET creates a greater energy density in a particle track and a higher average number of energy transfers to each critical volume located in that track. As discussed above, when the multiplicity of energy transfers to a critical volume is low, the result appears to enhance the probability of creating a break. However, when the multiplicity is high, energy is wasted since there can be no more than one break in a critical volume. Beyond the inflection point each incremental increase in LET becomes less effective and the curve in Figure 7 approaches a plateau. The effect of multiple energy transfers together with a fixed number of possible sites for breakage (determined by the overlap of track structure and chromatin fibers) results in a sigmoidal dose response from single particle traversals. The particle velocities used in the thesis work are well above the range where hooks have been observed in survival data (Kraft et al., 1985).

Initial Distribution of Chromatin Breaks

To assess the distribution of a certain kind of lesion in an irradiated cell population requires a technique that can detect that

lesion in individual cells. DNA strand break assays use a homogenate of a large number of cells so it is possible to determine only average values from the data. It is possible to construct distributions from chromosome aberration data. However, chromosome aberrations are remnant lesions persisting after extensive modification of the initial lesions by repair/misrepair processes and progression through the cell cycle. The PCC technique can detect one type of lesion, the chromatin break, in individual cells before substantial modification by cellular processes. It is, therefore, a useful method for investigating the distribution of these lesions.

Figure 9, which displays in histogram form 3 distributions obtained by using the PCC technique with CHO-tsH1 cells, clearly illustrates the effect of LET. The unirradiated control distribution is tightly dispersed. The x-ray histogram could be fitted well by a Poisson distribution as was indicated by a chi-squared "goodness-of-fit" statistical test. Its dispersion did not differ significantly from that of a Poisson distribution as shown by Fisher's dispersion test (Fisher, 1946). The histogram of PCC data obtained after exposing cells to 960 MeV/u uranium ions is also shown in Figure 9. In comparison to a theoretical Poisson distribution with the same mean as the uranium data, the histogram has the appearance of being overdispersed. Many cells had no detectable breaks while others had a large number of breaks per cell. The impression of overdispersion was clearly confirmed by the dispersion test. Results of a similar analysis of data from all 10 beams are presented in Table 4. With increasing LET there is a definite trend towards larger values of the relative dispersion. In general, low LET beams induce chromatin breakage in the irradiated cell population that does not differ significantly from a Poisson distribution, while the high LET-induced lesions are overdispersed. Overdispersion was attributed by

Tobias et al (1986) to the production of multiple chromatin breaks per cell from single high LET particle traversals. The number of particles passing through a cell nucleus was assumed to follow a Poisson distribution. Each particle was assumed to have a chance of breaking chromatin at any one of several track structure/chromatin fiber overlap regions. The number of overlap regions depended on track structure and the amount and distribution of DNA within the cell nucleus. Based on these considerations it was suggested that chromatin breaks follow a Neyman distribution among the cells. The Neyman distribution characteristicly is more widely dispersed than a Poisson of the same mean and, under certain circumstances, would predict peaks and valleys in the distribution of lesions. Virsik and Harder (1981) used a slightly different mathematical formalism to explain overdispersion of chromosome aberrations in mitotic cells that had been exposed to fast neutrons and $\alpha$-particles. Here too the effect was assumed to be due to multiple events per particle traversal. In their model of radiation effects, Kellerer and Rossi (1978) suggested that lesions and sublesions may not be Poisson distributed. Albright and Tobias (1985) have allowed for multiple lesions per particle track in a Markov version of the repair-misrepair model of cell survival.

Rejoining Kinetics

DNA strand break assays have shown that ionizing radiation induces single- and double-strand breaks in the DNA double helix. The same assays have demonstrated the existence of a cellular capacity for rejoining a portion of these breaks. Another portion remained unrejoined within the time frame of the experiments. Measured under alkaline conditions, Ritter et al (1977) and Roots et al (1979) found a LET-dependence for the unrejoined fraction of strand breaks. The presence of exchange-type chromosome aberrations in mitotic cells is an

indication of rejoining processes operating at the chromosomal level. Kraft et al (1985) observed a shift away from exchange-type aberrations at low LET to aberration types resulting from nonrejoining of chromosome breaks at high LET. The PCC technique demonstrates directly the breakage and rejoining of interphase chromosomes. Several investigations have shown that most chromatin breaks rejoin following x-rays (Cornforth and Bedford, 1987; Pantelias and Maillie, 1985). These studies, like the DNA strand-break studies, find that a small fraction of the initial breaks fail to rejoin. As part of the thesis work, the PCC studies were extended to cover a range of LET values.

Chromatin breaks in CHO-tsH1 cells exposed to particle beams were found to rejoin during post-irradiation incubation at 35°C (Fig. 10). The time course of the rejoining process could be adequately described by a two-component equation, Equation (1) (see Results section). The faster component is asumed to represent a fraction of the initial breaks that rejoin by first order kinetics. The time constant of the rejoining process did not appear to depend strongly on LET. For the 4 beams tested, Table 5 shows the values of parameters obtained by fitting the data to equation 1. Three of the 4 beams (H, Ar, and Ne-peak) led to time constants within $\pm$ 6% of 42 minutes while the fourth (C) had a time constant significantly larger than the others. The second component in equation (1) is assumed to be due to a fraction of the initial breaks that do not rejoin. The nonrejoining component showed a clear LET dependence. It increased 3.4 fold, from ~ 14 to 47% of total breaks, when the LET increased from ~ 0.56 to 183 keV/μm. The possibility cannot be excluded that some of the "nonrejoining" chromatin breaks might have rejoined had the experiments been extended to longer times.

Although it is not known why some chromatin breaks fail to rejoin, several possible explanations can be offered. 1. Ring chromosome

aberrations are created from the misrepair of two breaks on the same chromosome. The one original chromosome becomes two pieces, a ring plus a fragment, even though both breaks have rejoined. In a PCC assay, ring formation can lead to an overestimation of the number of breaks remaining after repair incubation. However the number of rings is too small to account for more than a small fraction of what are scored as nonrejoining breaks. In DNA strand-break assays, ring formation reduces the average size of DNA framents and, because of the higher doses often used, may significantly affect measurements of rejoining. 2. There may be a type of molecular product at the ends of some chromatin breaks that the cell is unable to remove. An example might be a DNA hairpin loop. 3. Unrejoinable breaks may result from multiply-damaged sites. For example, damage to chromosomal proteins at the site of a dsb or the creation of a gap in the chromatin fiber from two dsb in close proximity. This hypothesis is especially attractive in view of the observed LET dependence of nonrejoining breaks. If two or more energy transfers within a critical volume are necessary to create a multiply-damaged site then the curve formed by plotting nonrejoining breaks per cell per particle vs LET would be expected to have a slope of 2 in the sparsely ionizing region. Figure 18 shows the number of unrejoined chromatin breaks/cell/particle plotted vs LET. The curve has a slope of ~1.3. Nonrejoining DNA strand-break data can be converted to a relative effectiveness per particle traversal. Plotted this way the data of Ritter et al (1977) have a slope of 1 below 10 keV/μm and a slope of ~1.8 between 10 and 100 keV/μm. The data of Roots et al (1979) have a slope of ~2.3 below 60 keV/μm. Taken together these LET studies tend to argue in favor of a role for multiple damage in a particle track/chromatin fiber overlap region in the creation of nonrejoining breaks. To be convincing the argument will need to be supported by more data and might

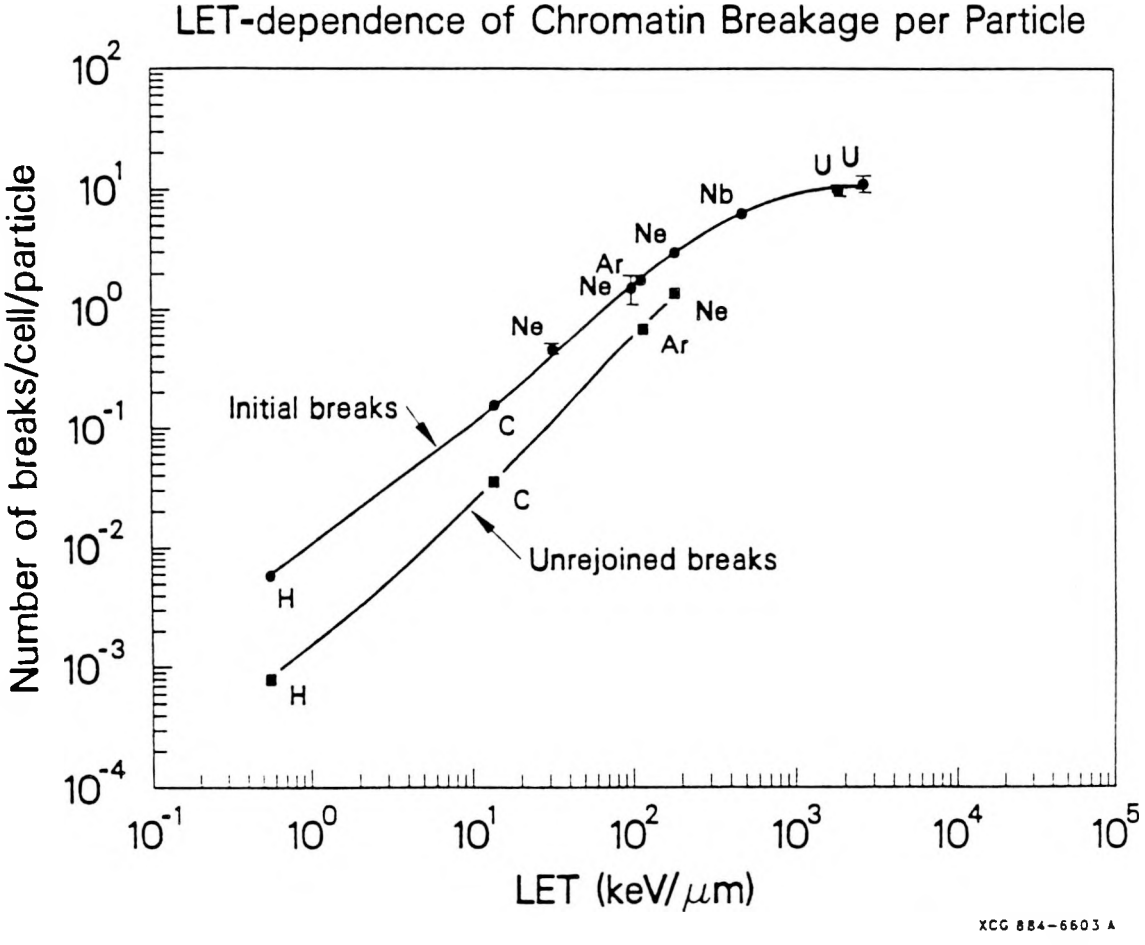


Figure 18. Chromatin breakage per single particle traversal both initially and after long incubation periods.

benefit from an application of the concepts and analytic tools of microdosimetry.

Chromatin break rejoining kinetics were also measured in UV24C2-3 cells exposed to high doses of x-rays and Ne-peak ions (Fig. 14). Compared to the CHO-tsH1 cell data, similar levels of unrejoined breaks were found after both the low- and high-LET radiations (11 and 49%, respectively). The two time constants for the rejoining process, 23.6 minutes for x-ray and 28.7 minutes for Ne-Peak, were similar. However, these time constants are much lower than those found in CHO-tsH1 cells. The difference may be due to cell line properties or to the slightly warmer temperature (37°C) used in the repair incubations. Also, after a high dose even with partial repair, difficulty in scoring the numerous PCC fragments present in each cell may lead to undercounting. This could make the rejoining rate appear to be faster than it actually is. It is possible that the rejoining of chromatin breaks is not a pure first order process but rather that the kinetics may possess a second order component. This too would make the rejoining rate appear to be faster after high doses if the data were fitted to equation (1).

Chromosomal Misrepair

A number of studies have demonstrated a LET dependence for chromosome aberrations scored in first post-irradiation mitoses (Skarsgard, et al, 1967; Geard 1985; Kraft et al, 1985; Ritter et al, 1987). These studies give no information on the initial level, or type, of lesion whose misrepair causes a chromosome aberration so it is not possible to investigate the kinetics of the misrepair process. DNA strand-break studies can measure the initial level of lesions and the kinetics with which they rejoin but do not distinguish repair from misrepair in the rejoining process. The PCC technique has rarely been used to investigate chromosomal misrepair kinetics in $G_1$ cells and had not been utilized in a

LET study. As part of the thesis work, ring PCC aberrations were scored in confluent, serum-deprived UV24C2-3 cells exposed to x-rays and Ne-peak ion beams at several post-irradiation time points.

Several interesting observations can be made regarding the kinetics of ring formation seen in this study. First, in the initial 2-3 hours following irradiation, Pantelias and Maillie (1985) found that chromatin break rejoining was not coupled to a simultaneous increase in ring aberrations in $G_0$ lymphocytes. This result implies that ring formation is not related to the extensive rejoining that takes place during this early time period. In contrast, the data presented in Figures 14 and 15 suggest that chromosomal repair and misrepair proceed simultaneously and it is reasonable to assume that they are two facets of the same rejoining process. Second, comparing their measurements of chromatin breakage to the double-strand DNA breakage data of Blocher and Pohlit (1982), Cornforth and Bedford (1983b; 1985) have noted that not all d.s. breaks are expressed as chromatin breaks. In the UV24C2-3 cell line only ~ 18% of d.s. breaks are observed as chromatin breaks in a PCC assay after x-irradiation. It has been suggested that the unexpressed d.s. breaks may represent a rapidly rejoining fraction of the initial breaks that has disappeared by the time the PCC procedure is complete. If this is so, the fast rejoining component of d.s. breaks cannot contribute significantly to ring aberration formation or else many more rings would have been observed at time t = 0 in the PCC assay. Third, a persistent question about the PCC technique has been how much repair takes place during the process itself before the zero-hour time point. By extrapolating the x-ray curve in Figure 15 back in time to a point where no rings are present, it can be estimated that an amount of repair (or misrepair) has taken place equivalent to what would occur in 5.5 minutes of incubation at 37°C. Fourth, if repair and misrepair of chromatin

breaks follow first order kinetics, then it would be expected that the time constants for rejoining and for ring formation would be the same. Results of this thesis demonstrate a substantial difference between the two time constants suggesting that chromosomal repair and misrepair may not be simple first order processes. The quadratic dependence on dose of the yield of rings at long repair times is another indication of complex kinetics. Fifth, as mentioned in the Results section the x-ray ring data obtained after long incubation intervals could be fitted by a quadratic dose-response curve (Equation 3) while the Ne ring data could be fitted equally well by either a linear or a quadratic curve. Assuming that the yield of rings follows a quadratic dose response for both x-rays and Ne ions, it is possble to fit the two data sets to an equation of the form $R = \beta(B_r)^2$ since $B_r$, the number of rejoinable breaks, scales at least approximately linearly with dose. The values obtained for the rate constants, $\beta$x-ray = $1.12 \times 10^{-4}$ and $\beta_{Ne} = 1.10 \times 10^{-4}$, are nearly the same. The probability for the misrepair of a rejoinable break appears to be independent of the LET of the radiation that produced it. This conclusion may be surprising at first. It might be expected that multiple chromatin breaks per particle traversal would lead to greater misrepair in the Ne experiments due to the proximity of lesions in particle tracks. However, with an average of only ~1.5 repairable breaks per particle and 20 to 40 particles per cell nucleus, intratrack misrepair may be of lesser importance than intertrack misrepair to the total yield of rings.

The conclusions stated above are based on an as yet small number of experiments. New techniques capable of gathering in a reasonable time much larger amounts of data on interphase chromosomal misrepair may be necessary to firmly establish (or refute) these conclusions. Nevertheless it may be profitable to examine other cellular endpoints of

radiation action, such as mutation and transformation, in terms of induced repairable chromatin breaks.

Chromosomal Damage, Repair and Misrepair and the LET-dependence of Cell Survival

Mammalian cells have an inherent ability to repair at least part of the damage caused by ionizing radiation. This capacity was discovered in clonogenic survival assays where either the plating of cells was delayed (Phillips and Tolmach, 1966) or the radiation exposures were fractionated (Elkind and Sutton, 1959). Because of its limitations, the survival assay has revealed little of the subcellular and molecular events involved in the damage and repair process. Radiation cytogenetics established a link between chromosome aberrations and loss of cellular reproductive capacity. This link has held over a wide LET range. The PCC technique made possible the investigation of chromosomal damage and repair while cells were still in interphase. Thus, from the first observations of clonogenic survival, the study of radiation-induced biological damage and the cellular response to that damage has been extended down to the subcellular level and backwards in time to within a few minutes of the actual radiation exposure. Attempts to correlate x-ray-induced chromosomal damage and repair with its ultimate expression in the operationally-defined cell-survival repair assays have already been fruitful (Cornforth and Bedford, 1987; Bedford and Cornforth, 1987). The purpose of this final section will be to examine the data gathered in the course of the thesis research in a search for insights into the LET-dependence of the survival response of cells exposed to accelerated particle beams.

Measurements of cell survival following exposure to radiations of increasing LET have demonstrated a progressive loss of the shoulder in survival curves (this thesis and see Review). Survival RBE values, with

some exceptions are generally found to reach a peak in the 100-200 keV/μm range. The magnitude of the RBE is influenced by several factors including survival level and inherent radiosensitivity of the cell line. Effects attributed to track structure have also been observed. PLD repair is greatest following the lowest LET radiations and is reduced or eliminated after high LET radiation exposures.

A number of studies have demonstrated a linear dose response for chromatin breakage induced by x-rays (see Review) while this thesis has shown that these low LET lesions are Poisson distributed among the cells. If the chromatin break is the lesion whose misrepair or nonrepair is responsible for loss of clonogenic capacity, then it should be possible to quantitatively relate events occurring at the chromosomal level to cell survival measurements. Without repair of chromatin breaks, a CHO-tsH1 x-ray survival curve would be exponential. The surviving fraction would be reduced to 37% after only a 14 rad dose, a point where there is an average of 1 break per cell. Comparison with the experimentally determined survival curve (Fig. 3) suggests that much repair must take place even after immediate plating. Furthermore, the curvature of the survival response is an indication of decreasing repair effectiveness with increasing dose. Assuming that the lethal lesions (asymmetrical exchanges and chromosomal deletions) are also Poisson distributed, then at the 50% survival level ~23 of 24 initial chromatin breaks are repaired, or at least rendered nonlethal, while at the 1% level the frequency of repair has been more than halved to 10 of 11 breaks. Delayed plating of CHO-tsH1 cells after 770 rad x-ray exposures results in a 2.4 fold increase in survival from 1% to 2.4% (Fig. 4). Of an average of 56.6 initial chromatin breaks per cell, ~4.6 become lethal lesions at some time after immediate plating. With repair incubation this number is reduced to ~3.7. While the increase in survival is

substantial, PLD repair affects less than 2% of the initial chromatin breaks and appears to represent only a small increase over the amount of repair that would take place even with immediate plating.

The survival response of cells exposed to particle beams is likely to be influenced by several features of the LET dependence of interphase chromosomal breakage, rejoining and misrepair. These are: 1. The initial level of chromatin breakage is LET dependent (Fig. 6). This property of particle beam irradiation could account for major characteristics of the survival RBE vs LET curve such as the existence and position of a peak and the progressive decline following the peak. Figure 19 shows survival RBE vs LET curves for several survival levels and also the chromatin breakage vs LET curve for CHO-tsH1 cells. As the survival level decreases, the survival RBE curve appears to collapse downwards until at the 1% level it is almost indistinguishable from the chromatin breakage RBE curve. Experiments performed in the course of the thesis research were not designed to test survival below the 1% level so it is not possible to say with certainty how the RBE curve would behave at even lower survival levels. In this context it is interesting to compare predictions made by various cell survival models. A model that results in a linear-quadratic survival curve (Chadwick and Leenhouts, 1973) would predict that as $S \to 0$ the RBE approaches $\sqrt{\beta(\text{ion})/\beta(\text{x-ray})}$ as a limit where $\beta$ is the coefficient of the quadratic term in the survival equation. In this model the limiting RBE can become vanishingly small because $\beta(\text{ion}) \sim 0$ in the high LET range. The single-hit-multitarget model (Lea, 1956) predicts that the RBE approaches $D_o(\text{x-ray})/D_o(\text{ion})$, where $D_o$ refers to the inverse of the slope of the exponential portion of the survival curve. It is difficult to relate this prediction to chromatin breakage in a meaningful way. In the low survival limit, the Repair-Misrepair (RMR) model (Tobias et al, 1980) predicts that the RBE

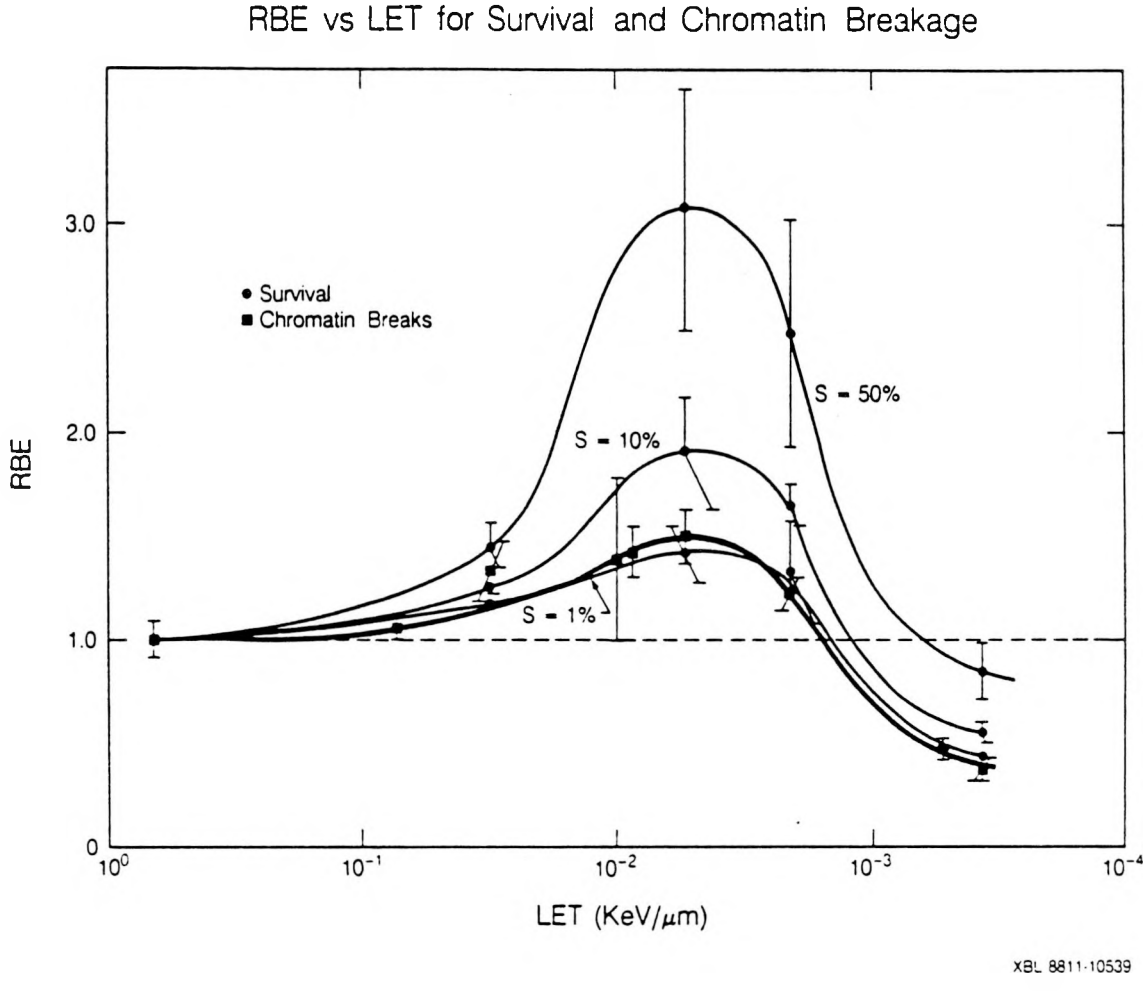


Figure 19. Comparison between the survival RBE computed at three survival levels and the chromatin-breakage RBE.

approaches $\delta(ion)/\delta(x\text{-ray})$, where $\delta$ is the rate constant for the linear induction of initial "uncommitted" lesions. If chromatin breaks can be equated to uncommitted lesions, then the RMR model predicts that the survival RBE would collapse to the chromatin breakage RBE. In addition a plausible explanation follows from the RMR model. Low survival requires high doses that produce a large number of initial lesions. Under these circumstances "quadratic" misrepair dominates "linear" eurepair causing cellular repair mechanisms to become ineffective. In this case survival will depend only on the initial number of lesions. Although the LET dependence of chromatin breakage can account for the overall shape of the survival RBE vs LET curve it does not explain the loss of a shoulder in high LET survival curves. 2. The initial distribution of chromatin breaks within the irradiated cell population becomes progressively overdispersed as the LET increases. This phenomenon is intimately linked to the production of multiple chromatin breaks by single particle traversals of the cell nucleus. The effect on cell survival of overdispersion of lesions was examined by Albright and Tobias (1985) within the framework of the RMR model. Their analysis attempted to account for variances in the number of tracks through a nucleus, the type of particle, the LET, the track length due to the shape of the nucleus, and the amount of DNA per cell due to aneuploidy - all of which have an effect on the distribution of lesions. It was concluded that these effects decrease the cell-killing potential of particle beams. 3. As LET increases so does the proportion of nonrejoining chromatin breaks. This feature of LET-dependent chromatin breakage affects the survival response by rendering chromosomal repair mechanisms increasingly ineffective. Therefore it is expected, and observed, that as LET increases survival curves lose their shoulders and PLD repair is diminished. It is interesting to note that radiosensitive AT cells fail to rejoin a large

fraction of initial chromatin breaks when exposed to x-rays (Cornforth and Bedford, 1985) and so behave somewhat like normal cells exposed to high LET particle beams. 4. Misrepair at the chromosomal level, as manifested in the creation of exchange-type aberrations, is likely to play a lesser role in the high LET range due to the increasing proportion of nonrejoining chromatin breaks. Both the chromosome aberration data of Kraft et al (1985) and measurements of ring-PCC aberrations presented in this thesis support such a conjecture. The survival response to high LET irradiation may be influenced less by repair-misrepair processes and more by the absolute number and distribution of nonrejoining chromatin breaks.

# APPENDIX

## Growth Medium (CHO)

Minimal Essential Medium (MEM)
with Earle's Salts (Gibco)
0.25 mg/ml L-Glutamine (Gibco)
43 Units/ml Potassium Penicillin
(M.A. Bioproducts)
1.94 mg/ml $NaHCO_3$ (Gibco
0.31mM MEM Non-Essential
Amino Acid Solution (Gibco)
10% Fetal Bovine Serum

## Growth Medium (UV24C2-3)

Alpha MEM
10% Fetal Bovine Serum
0.44 mg/ml L-glutamine
43 units/ml Potassium
Penicillin

## Fusogen (UV24C2-3)

51.6% Polyethylene Glycol
MW 1000 (Sigma)
48.4% 120 mM Hepes

## Selection Medium

Growth Medium
10µg/ml Mycophenolic
Acid (Calbiochem)
10µg/ml Thymidine
25µg/ml Adenine
250µg/ml Xanthine
0.25µg/ml Methotrexate
(Sigma)

## Wash Solution

Hank's Balanced Salt Solution
(Gibco)
0.4 mM $MnCl_2$
0.2 mM ATP (Sigma)
25 µg/ml Cycloheximide
2 µg/ml Colchicine

## Freezing Medium (CHO-MB)

CHO Growth Medium
5% Fetal Bovine Serum
(Additional)
17 mM Pipes
2 µg/ml Colchicine
4% DMSO

## PCC Medium

McCoy's 5a Medium (Gibco)
15% Fetal Bovine Serum
0.5 mM $MgCl_2$
0.5 mM $MnCl_2$
1 mM Spermine
0.5 mM ATP
0.38 mg/ml $NaHCO_3$ (Gibco)
25 µg/ml Cycloheximide
2.5 µg/ml Colchicine
13 Units/ml Potassium
Penicillin (M.A. Bioproducts)

## Thawing Medium

50% Growth Medium
50% PCC Medium

## Sorensen's Buffer (pH 6.8)

25.5% 0.2 M $NaH_2PO_4.H_2O$

74.5% 0.656 M $NaH_2PO_4.12H_2O$

REFERENCES

Albright, N. (1987), Computer Programs for the Analysis of Cellular Survival Data, Radiation Res 112: 331-340.

Albright, N. (1988), A User's Guide to Computer Programs for the Analysis of Cellular Survival Data, Lawrence Berkeley Laboratory Publication No. 22347.

Albright, N.W. and C.A. Tobias (1985), Extension of the Time-Independent Repair-Misrepair Model of Cell Survival to High-LET and Multicomponent Radiation, Proceedings of the Berkeley Conference in Honor of Jerzy Neyman and Jack Kiefer (L. LeCam and R. Olshen, eds), 397-424, Wadsworth, Inc.

Amols, H.I., B. Lagueux and D. Cagna (1986), RBE of Megavoltage X-Ray and Electron Beams in Radiotherapy, Radiation Res. 105: 58-67.

Athwal, R.S., M. Smarsh, B.M. Searle and S.S. Deo (1985), Integration of a Dominant Selectable Marker Into Human Chromosomes and Transfer of Marked Chromosomes to Mouse Cells by Microcell Fusion, Somatic Cell and Molecular Genetics 11: 177-187.

Aufderheide, E., H. Rink, L. Hieber and G. Kraft (1987), Heavy Ion Effects on Cellular DNA, Int. J. Radiat. Biol. 51: 779-790.

Barendsen, G.W., H.M.D. Walter, J.F. Fowler and D.K. Bewley (1963), Effects of Different Ionizing Radiations on Human Cells in Tissue Culture, Radiation Res. 18 106-119.

Barendsen, G.W., C.J. Koot and G.R. Van Kersen (1966), The Effect of Oxygen on Impairment of the Proliferative Capacity of Human Cells in Culture by Ionizing Radiations of Different LET, Int. J. Rad. Biol. 10: 317-327.

Bedford, J.S. and M.N. Cornforth (1987), Relationship Between the Receovery from Sublethal X-Ray Damage and the Rejoining of Chromosome Breaks in Normal Human Fibroblasts, Radiation Res. 111: 406-423.

Bedford, J.S. and D.T. Goodhead (1987), Breakage of Human Interphase Chromosomes by Alpha Particles, 8th International Congress of Radiation Research Abstract D51-10p.

Berry R.J. (1977), Reproductive Survival and Hypoxic Protection as a Function of Radiation Ionization Density, Radiation Res 10: 355-361.

Bevalac User's Handbook (1977), Lawrence Berkeley Laboratory, Biology and Medicine Division Publication 101.

Biological and Medical Research with Accelerated Heavy Ions at the Bevalac, 1977-1980 (M.C. Pirrucello and C.A. Tobias, eds), LBL Publication 11220.

Blakely, E.A., P.Y. Chang and L. Lommel (1985), Cell-Cycle-Dependent Recovery From Heavy-Ion Damage in $G_1$-Phase Cells, Radiation Res. 104: S-145-147.

Blakely, E.A., F.Q.H. Ngo, S.B. Curtis and C.A. Tobias (1984), Heavy-Ion Radiobiology: Cellular Studies, Adances in Radiation Biology, 11: 295-389.

Blakely, E.A., C.A. Tobias, T.C.H. Yang, K.C. Smith and J.T. Lyman (1979), Inactivation of Human Kidney Cells by High-Energy Monoenergetic Heavy-Ion Beams, Radiation Res. 80: 122-160.

Blocher, D. and W. Pohlit (1982), DNA Double Strand Breaks in Ehrlich Ascites Tumor Cells at Low Doses of X-Rays, Int. J. Radiat. Biol. 42: 329-338.

Bryant, P.E. (1984), Enzymatic-Restriction of Mammalian Cell DNA Using Pvu II and Bam H1: Evidence for the Double-Strand Break Origin of Chromosomal Aberrations, Int. J. Radiat. Biol. 46: 57-65.

Carrano, A.V. (1973), Chromosome Aberrations and Radiation-Induced Cell Death, Mutation Res 17: 355-366.

Carrano, A.V. and J.A. Heddle (1973), The Fate of Chromosome Aberrations, J. Theor. Biol. 38: 289-304.

Chadwick, K.H. and H.P. Leenhouts (1973), A Molecular Theory of Cell Survival, Physics Med. Biol. 18: 78-87.

Chatterjee, A., H.D. Maccabee and C.A. Tobias (1973), Radial Cutoff LET and Radial Cutoff Dose Calculations for Heavy Charged Particles in Water, Radiat. Res. 54: 479-494.

Chatterjee, A. and J.L. Magee (1980), Energy Transfer from Heavy Particles, LBL Publication 11220, p. 53.

Chatterjee, A. and H.J. Schaefer (1976), Microdosimetric Structure of Heavy-Ion Tracks in Tissue, Rad. and Environm. Biophys. 13: 215-227.

Christensen, R.C., C.A. Tobias and W.D. Taylor (1972), Heavy-ion-induced Single- and Double-strand Breaks in $\phi$X174 Replicative Form DNA, Int. J. Radiat. Biol. 22: 457-477.

Conger, A.D., M.L. Randolph, C.W. Sheppard and H.J. Luippold (1958), Quantitative Relation of RBE in Tradescantia and Average LET of Gamma-rays, X-rays, and 1.3-, 2.5-, and 14.1-MeV Fast Neutrons, Radiat. Res. 9: 525-547.

Cornforth, M.N. and J.S. Bedford (1983a), High-Resolution Measurement of Breaks in Prematurely Condensed Chromosomes by Differential Staining, Chromosoma 88: 315-318.

Cornforth, M.N. and J.S. Bedford (1983b), X-Ray Induced Breakage and Rejoining of Human Interphase Chromosomes, Science 222, 1141-1143.

Cornforth, M.N. and J.S. Bedford (1985), On the Nature of A Defect in Cells from Individuals with Ataxia Telangiectasia, Science 227: 1589-1591.

Cornforth, M.N. and J.S. Bedford (1987), A Quantitative Comparison of Potentially Lethal Damage Repair and the Rejoining of Interphase Chromosome Breaks in Low Passage Normal Human Fibroblasts, Radiat. Res. 111, 385-405.

Cox, R., J. Thacker, D.T. Goodhead and R.J. Munson (1977), Mutation and Inactivation of Mammalian Cells by Various Ionizing Radiations, Nature 267: 425-427.

Croxton, F.E. (1953), Elementary Statistics, Dover Publications, Inc., New York: 288-291.

Curtis, S.B. and W. Schimmerling, Nuclear Physics of Accelerated Heavy Ions, Biological and Medical Research with Accelerated Heavy Ions at the Bevalac 1974-1977 Ch 4: 36-46.

Das, N.K. and M. Alfert (1961), Accelerated DNA Synthesis in Onion Root Tip Meristem During X-irradiation, Proc. Natl. Acad. Sci. 47: 1-6.

Dewey, W.C., H.H. Miller and D.B. Leeper (1971), Chromosomal Aberrations and Mortality of X-Irradiated Mammalian Cells: Emphasis on Repair, Proc. Natl. Acad. Sci 68: 667-671.

Edwards, A.A., D.C. Lloyd and R.J. Purrott (1979), Radiation Induced Chromosome Aberrations and the Poisson Distribution, Rad. and Environm. Biophys. 16: 89-100.

Elkind, M.M. and H. Sutton (1959), X-Ray Damage and Recovery in Mammalian Cells in Culture, Nature 184: 1293-1295.

Evans, R.D. (1955), The Atomic Nucleus, Ch 18, McGraw-Hill, New York.

Fisher, R.A. (1946), Statistical Methods For Research Workers 10th Ed. Hafner Publishing Co., New York: 58.

Geard, C.R. (1985), Charged Particle Cytogenetics: Effects of LET, Fluence, and Particle Separation on Chromosome Aberrations, Radiation Res. 104: S-112-S-121.

Giles, N.H. and C.A. Tobias (1954), Effect of LET on Radiation-induced Chromosome Aberrations in Tradescantia Microspores, Science 120: 993-994.

Gragg, R.L., R.M. Humphrey and R.E. Meyn (1977), The Response of Chinese Hamster Ovary Cells to Fast-Neutron Radiotherapy Beams, Radiation Res. 71: 461-470.

Grote, S.J., G.P. Joshi, S.H. Revell and C.A. Shaw (1981), Observations of Radiation-Induced Chromosome Fragment Loss in Live Mammalian Cells in Culture, and Its Effect on Colony-Forming Ability, Int.J. Radiat. Biol. 39: 395-408.

Hall, E.J., J.K. Novak, A.M. Kellerer, H.H. Rossi, S. Marino and L.J. Goodman (1975), RBE As A Function of Neutron Energy, Radiation Res 64: 245-255.

Harris, H. and J.F. Watkins (1965), Hybrid Cells Derived From Mouse and Man, Nature 205: 640-646.

Hermann, J., O. Mulner, R. Belli, J. Marot, J. Tso and R. Ozon (1984), In Vivo Effects of Microinjected Alkaline Phosphatase, Proc. Natl. Acad. Sci. 81: 5150-5154.

Hieber, L. and C. Lucke-Huhle (1983), PCC Technique Reveals Severe Chromatin Lesions and Repair in $G_2$ - Arrested Cells After Alpha Irradiation. Exp. Cell Res. 144: 57-67.

Hittelman, W.N. and M. Pollard (1982), A Comparison of the DNA and Chromosome Repair Kinetics After $\gamma$ Irradiation, Radiation Res. 92: 497-509.

Hittleman, W.N. and P.N. Rao (1974), Premature Chromosome Condensation II. The Nature of Chromosome Gaps Produced by Alkylating Agents and Ultraviolet Light, Mutation Research 23: 259-267.

Iliakis, G., G.E. Pantelias and R. Seaner (1988), Effect of Arabinofuranosyladenine on Radiation-Induced Chromosome Damage in Plateau-Phase CHO Cells Measured by PCC: Implications for Repair and Fixation of $\alpha$-PLD, Radiation Res. 114: 361-378.

Johnson, R.T. and P.N. Rao (1970), Mammalian Cell Fusion II. Induction of Premature Chromosome Condensation in Interphase Nuclei, Nature 226: 717-722.

Johns, H.E. and J.R. Cunningham (1974), The Physics of Radiology, Third Edition, Charles C. Thomas Publisher, Springfield, Illinois.

Joshi, G.P., W.J. Nelson, S.H. Revell and C.A. Shaw (1982), X-Ray-Induced Chromosome Damage in Live Mammalian Cells, and Improved Measurements of Its Effects on Their Colony-Forming Ability, Int. J. Radiat. Biol. 41: 161-181.

Kampf, G. and K. Eichhorn (1983), DNA Strand Breakage by Different Radiation Qualities and Relations to Cell Killing, Studia Biophysisica 93: 17-26.

Katz, R. (1978), Track Structure Theory in Radiobiology and in Radiation Detection, Nuclear Track Detection Vol. 2, No. 1: 1-28.

Kellerer, A.M. and H.H. Rossi (1978), A Generalized Formulation of Dual Radiation Action, Radiation Res 75: 471-488.

Klebe, R.J. and M.G. Mancuso (1981), Chemicals Which Promote Cell Hybridization, Somatic Cell Genetics 7: 473-488.

Kraft, G.H., E.A. Blakely, W. Kraft-Weyrather, P.Y. Chang, L. Lommel, R. Roots, T.C.H. Yang, L.M. Craise, M. Mei, M. Wong, M. Rapkin, W. Schimmerling, J. Howard, M.J. Yezzi, J. Schmidt, and C.A. Tobias (1985), Super Heavy Ions: Uranium Radiobiology and Physics, LBL Publication 13893, 128-137.

Kraft, G., W. Kraft-Weyrather and A. Lang (1987), Abstract B5 Third Workshop on Heavy Charged Particles in Biology and Medicine, G.S.I. Report 87-11.

Lea, D.E. (1956), Actions of Radiation on Living Cells, Second Edition, Cambridge University Press, London and New York.

Little, J.B. and H. Nagasawa (1985), Effect of Confluent Holding on Potentially Lethal Damage Repair, Cell Cycle Progression and Chromosomal Aberrations in Human and Ataxia-Telangiectasia Fibroblasts Radiat. Res. 101: 81-93.

Madhvanath, V., M.R. Raju and L.S. Kelly (1976), Survival of Human Lymphocytes After Exposure to Densely Ionizing Radiation, In Radiation and the Lymphatic System Conf-740930, USERDA Technical Information Service, Oak Ridge, Tennessee.

Natarajan, A.T., Obe, G (1978), Molecular Mechanisms Involved in the Production of Chromosomal Aberrations. 1. Utilization of Neurospora Endonuclease for the Study of Aberration Production in G2 State of the Cell Cycle, Mutat Res 52: 137-149.

Natarajan, A.T., and G. Obe (1984), Molecular Mechanisms Involved in the Production of Chromosomal Aberrations III. Restriction Endonucleases, Mutat. Res 90: 120-127.

Neary, G.J. (1965), Chromosome Aberrations and the Theory of RBE I, Int. J. Rad. Biol. 9: 477-502.

Neary, G.J. and J.R.K. Savage (1966), Chromosome Aberrations and the Theory of RBE II, Int. J. Rad. Biol. 11: 209-223.

Ngo, F.Q.H., E.A. Blakely and C.A. Tobias (1981), Sequential Exposures of Mammalian Cells to Low- and High-LET Radiations, Radiation Res 87: 59-78.

Ngo, F.Q.H., E.A. Blakely and T.C.H. Yang, M.J. Yezzi and C.A. Tobias (1980), Cellular Damage and Repair Following Heavy-Ion Irradiation, LBL Publication 11220, 89-102.

Obara, Y, H. Yoshida, L.S. Chai, H. Weinfield and A.A. Sandberg (1973), Contrast Between the Environmental pH Dependence of Prophasing and Nuclear Membrane Formation in Interphase - Metaphase Cells, J. Cell Biology 58: 608-617.

Obara, Y., L.S. Chai, H. Weinfield and A.A. Sandberg (1974), Prophasing of Interphase Nuclei and Induction of Nuclear Envelopes Around Metaphase Chromosomes in HeLa and Chinese Hamster Homo- and Heterokaryons, J. Cell Biol. 62: 104-113.

Panetlias, G.E. (1986), Radiation-Induced Cytogenetic Damage in Relation to Changes in Interphase Chromosome Conformation, Radiation Res. 105: 341-350.

Pantelias, G.E. and H.D. Maillie (1983), A Simple Method for Premature Chromosome Condensation Induction in Primary Human and Rodent Cells Using Polyethylene Glycol, Somat. Cell Genet. 9: 533-547.

Pantelias, G.E. and H.D. Maillie (1985), Direct Analysis of Radiation-Induced Chromosome Fragments and Rings in Unstimulated Human Peripheral Blood Lymphocytes by Means of the Premature Chromosome Condensation Technique, Mutat. Res. 149, 67-72.

Perry, P. and S. Wolff (1974), New Giemsa Method for the Differential Staining of Sister Chromatids, Nature 251: 156-158.

Phillips, R.A. and L.J. Tolmach (1966), Repair of Potentially Lethal Damage in X-Irradiated HeLa Cells, Radiat. Res. 29: 413-432.

Pinkel, D., T. Straume and J.W. Gray (1986), Cytogenetic Analysis Using Quantitative High-Sensitivity, Fluorescence Hybridization, Proc. Natl. Acad. Sci. 83: 2934-2938.

Preston, R.J. (1982), DNA Repair and Chromosome Aberrations: Interactive Effects of Radiation and Chemicals, in: Natarajan AT. Obe G, Altmann H (eds) DNA Repair, Chromosome Alterations and Chromatin Structure. Elsevier Biomedical Press, pp 25-35

Puck, T.T. (1958), Action of Radiation on Mammalian Cells, Genetics 44: 772-780.

Puck, T.T. and P.I. Marcus (1956), Action of X-Rays on Mammalian Cells, J. Exp. Med. 103: 653-666.

Puck, T.T., S.J. Cieciura and A. Robinson (1958), Genetics of Somatic Mammalian Cells, J. Exp. Med. 108: 945-956.

Raju, M.R., J.P. Frank, E. Bain, T.T. Trujillo and R.A. Tobey (1977), Repair of Potentially Lethal Damage in Chinese Hamster Cells After X and $\alpha$-Irradiation Radiation Res. 71: 614-621.

Rao, P.N. and R.T. Johnson (1971), Mammalian Cell Fusion IV: Regulation of Chromosome Formation From Interphase Nuclei by Various Chemical Compounds, J. Cell. Physiol. 78: 217-224.

Revell, S.H. (1955), In "Proceedings of the Radiobiology Symposium, Liege, 1954" Z.M. Bacq and P. Alexander, eds., 243-253, Butterworth, London.

Ritter, M.A., J.E. Cleaver and C.A. Tobias (1977), High-LET Radiations Induce a Large Proportion of Non-Rejoining DNA Breaks, Nature 266: 653-655.

Ritter, S., W. Kraft-Weyrather, M. Scholz and G. Kraft (1987), Chromosome Aberrations Induced by Heavy Charged Particles, Abstract D15 Third Workshop on Heavy Charged Particles in Biology and Medicine, G.S.I. Report 87-11.

Roberts, C.J. and P.D. Holt (1985), Induction of Chromosome Aberrations and Cell Killing in Syrian Hamster Fibroblasts by $\gamma$-Rays, X-Rays and Fast Neutrons, Int. J. Radiat. Biol. 48: 927-939.

Roots, R., T.C. Yang, L. Craise, E.A. Blakely and C.A. Tobias (1979), Impaired Repair Capacity of DNA Breaks Induced in Mammalian Cellular DNA by Accelerated Heavy Ions, Radiation Res. 78: 38-49.

Sabatier, L., W.A. Achkar, F. Hoffscher, C. Luccioni and B. Dutrillaux (1987), Qualitative Study of Chromosomal Lesions Induced by Neutrons and Neon Ions in Human Lymphocytes at $G_o$ Phase, Mutation Res 178: 91-97.

Sax, K (1940), An Analysis of X-Ray Induced Chromosomal Aberrations in Tradescantia, Genetics 25: 41-68.

Sax, K (1941), The Behavior of X-Ray-Induced Chromosomal Aberrations in Allium Root Tip Cells, Genetics 26: 418-425.

Skarsgard, L.D., B.A. Kihlman, L. Parker, C.M. Pujara and S. Richardson (1967), Survival, Chromosome Abnormalities and Recovery in Heavy-Ion- and X-Irradiated Mammalian Cells, Radiation Res. Suppl. 7: 208-221.

Stadler, L.J. (1931), The Experimental Modification of Heredity in Crop Plants I. Induced Chromosomal Irregularities, Sci. Agr. 11: 557-572.

Sunkara, P., D.A. Wright and P.N. Rao (1979), Mitotic Factors from Mammalian Cells: A Preliminary Characterization, J. Supramolecular Structure 11: 189-195.

Teissie, J., V.P. Knutson, T.Y. Tsong amd M.N. Lane (1982), Electric PulseInduced Fusion of 3T3 Cells in Monolayer Culture, Science 216: 537-538.

Terasima, T. and L.J. Tolmach (1961), Changes in X-ray Sensitivity of HeLa Cells During the Division Cycle, Nature 190: 1210-1211.

Thompson, L.H., J.L. Harkins and C.P. Stanners (1973), A Mammalian Cell Mutant with a Temperature-Sensitive Leucycl-Transfer RNA Synthetase, Proc. Natl. Acad. Sci. 70: 3094-3098.

Tobias, C.A., E.A. Blakely, F.Q.H. Ngo and T.C.H. Yang (1980), The Repair-Misrepair Model of Cell survival, Radiation Biology in Cancer Research, (R.W. Meyn and H.R. Withers, eds.), 195-230, Raven Press, New York.

Tobias, C.A., E.A. Blakely, P.Y. Chang, L. Lommel and R. Roots (1984), Response of Sensitive Human Ataxia and Resistant T1 Cell Lines to Accelerated Heavy Ions, Br. J. Cancer 49, Suppl. VI: 175-185.

Tobias, C.A., E.H. Goodwin and E.A. Blakely (1986), DNA Lesions in Cell Nuclei Follow Neyman A Distribution, Lawrence Berkeley Laboratory Report Number 22300.

Todd, P.W. (1964), Reversible and Irreversible Effects of Ionizing Radiations on the Reproductive Integrity of Mammalian Cells Cultured In Vitro, Ph.D. Thesis, University of California, Berkeley.

Virsik, R.P. and D. Harder (1981), Statistical Interpretation of the Overdispersed Distribution of Radiation-Induced Dicentric Chromosome Aberrations at High LET, Radiation Res. 85: 13-23,

Waldren, C.A. and R.T. Johnson (1974), Analysis of Interphase Chromosome Damage by Means of Premature Chromosome Condensation after X- and Ultraviolet Irradiation, Proc. Natl. Acad. Sci. USA 71: 1137-1141.

Wolff, S. (1972), The Repair of X-ray-induced Chromosome Aberrations in Stimulated and Unstimulated Human Lymphocytes, Mutat. Res. 15: 435-444.

Wu, M. and J.C. Gerhart (1980), Partial Purification and Characterization of the Maturation-Promoting Factor from Eggs of Xenopus Laevis, Developmental Biol. 79: 465-477.